Modular Reactive Neurocontrol for Biologically Inspired Walking Machines

Poramate Manoonpong
Fraunhofer Institut für Autonome Intelligente Systeme (AIS), Sankt Augustin, Germany. Bernstein Center for Computational Neuroscience (BCCN), University of Göttingen, Germany
poramate@nld.ds.mpg.de

Frank Pasemann
Fraunhofer Institut für Autonome Intelligente Systeme (AIS), Sankt Augustin, Germany
frank.pasemann@ais.fraunhofer.de

Hubert Roth
Institut für Regelungs und Steuerungstechnik (RST), University of Siegen, Germany.
hubert.roth@uni-siegen.de

Abstract

A neurocontroller is described which generates the basic locomotion and controls the sensor-driven behavior of a four-legged and a six-legged walking machine. The controller utilizes discrete-time neurodynamics, and is of modular structure. One module is for processing sensor signals, one is a neural oscillator network serving as a central pattern generator, and the third one is a so-called velocity regulating network. These modules are small and their structures and their functionalities are analyzable. In combination, they enable the machines to autonomously explore an unknown environment, to avoid obstacles, and to escape from corners or deadlock situations. The neurocontroller was developed and tested first using a physical simulation environment, and then it was successfully transferred to the physical walking machines. Locomotion is based on a gait where the diagonal legs are paired and move together, e.g. trot gait for the four-legged walking machine and tripod gait for the six-legged walking machine. The controller developed is universal in the sense that it can easily be adapted to different types of even-legged walking machines without changing the internal structure and its parameters.

KEY WORDS—autonomous robots, walking machines, recurrent neural networks, neural control, reactive behavior

1. Introduction

Attempts to create autonomous mobile robots that can interact with their environments or can even adapt to specific survival conditions have been ongoing for over 50 years (Anderson and Donath 1988; Brooks and Stein 1994; Consi et al. 1995; Floreano and Mondada 1994; Hagras et al. 2000; Moravec 1977; Nehmzow and Walker 2003; Nilsson 1969; Nolfi and Floreano 1998; Payton 1986; Pfeifer and Scheier 1999). There are several reasons for this which can be summarized as follows: (1) such robotic systems can be used as models to test hypotheses regarding the information processing and control of the systems (Fend et al. 2003; Goerke et al. 2005; Okada et al. 2003; Schmucker et al. 2005); (2) they can serve as a methodology for studying embodied systems consisting of sensors and actuators for explicit agent–environment interactions (Hafner 2004; Hülse et al. 2003; Kimura and Fukuoka 2004; Wischmann et al. 2006); (3) they can stimulate the interaction between biology and robotics, i.e. biologists can use robots as physical models of animals to address specific biological questions, while roboticists can formulate intelligent behavior in robots by utilizing biological studies (Dürr et al. 2004; Ritzmann et al. 2004; Webb 2000).

The reasons given above show that the principle of creating agent–environment interactions combines various fields of study, e.g. the investigation of the robotic behavior control and understanding how a biological system works. It is also the basis for the achievement of a so-called "Autonomous Intelligent System" which still is a challenging task. Thus, the work described here continues in this tradition by using biologically inspired walking machines as agents. They are reasonably complex mechatronic systems which have to be controlled by more advanced techniques.

The concept of reactive control (Arkin 1998) is applied to generate the behavior of physical four- and six-legged walk-

The International Journal of Robotics Research
Vol. 26, No. 3, March 2007, pp. 301–331
DOI: 10.1177/0278364906076263

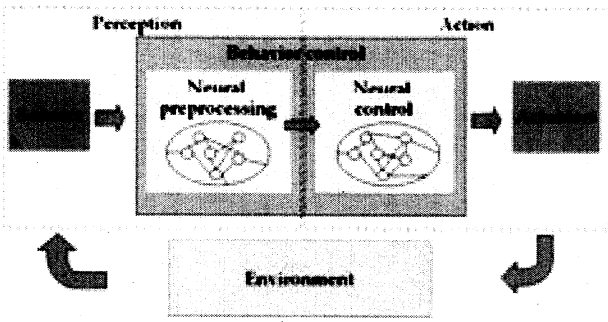

Fig. 1. Diagram of the modular reactive neural control. The controller acts as an artificial perception-action system, i.e. the sensor signals go through the neural preprocessing module into the neural control module, which commands the actuators. As a result, the robot's behavior is generated by the interaction with its (dynamic) environment in the sensorimotor loop.

ing machines; i.e. they can react to real environmental stimuli using only their sensor signals, but have no task planning algorithm or memory capacities. A reactive behavior controller, based on a modular structure, is modelled with an artificial neural network using discrete-time dynamics. A part of the controller is developed by realizing dynamical properties of recurrent neural networks. They exhibit several interesting dynamical properties (Pasemann 2002) which can be applied to create neural signal preprocessing and control. The modular reactive neurocontroller introduced here consists of two main modules: the neural preprocessing network and the neural control network, which is composed of a neural oscillator network and the velocity regulating networks (VRNs) (see Figure 1).

The function of this kind of a neurocontroller is easier to analyze than many others which have been developed for walking machines, for instance using an evolutionary technique (Filliat et al. 1999; Jacobi 1998; Parker and Lee 2003; Reeve 1999). In general, they are too large to be mathematically analyzed in detail, in particular if they use a massive recurrent connectivity structure. Furthermore, for most of these controllers it is almost *impossible* to transfer them successfully onto walking machines of different types, or to generate different walking modes (e.g. forwards, backwards, turning left and right motions) *without modifying the network's internal parameters or structure* (Beer 1990; Berns et al. 1994; Cruse et al. 2004; Yamaguchi et al. 2005.

In contrast, the controller developed here can be *successfully applied to a physical four- as well as to a six-legged walking machine*, and it is also able *to generate different walking modes without altering internal parameters or the structure of the controller*. Because the functionality of the modules is well understood, the reactive behavior controller of a less complex agent[1] (four-legged walking machine) can be applied also to a more complex agent (six-legged walking machine) and vice versa. And, it is also possible by a simple modification of the neural preprocessing module, to generate a different reactive behavior, e.g. sound tropism (positive tropism) (Manoonpong et al. 2004, 2005).

In this article, the neurocontroller is designed to enable the walking machines to avoid obstacles (negative tropism) by changing the rhythmic leg movements of the thoracic joints. Furthermore, it also prevents the walking machines from getting stuck in corners or deadlock situations by applying hysteresis effects provided by the recurrent structure of the neural preprocessing module. However, there is no appropriate benchmark for judging the success or failure of the systems. Therefore, we estimate the capability of the systems by empirical investigation and by actually observing their performance.

The following section describes the technical specifications of the walking machines together with their physical simulators. Section 3 explains the modular reactive neurocontroller together with its subnetworks (modules) for an obstacle avoidance behavior. The experiments and results are shown in Section 4. Discussion and conclusions are given in Sections 5 and 6, respectively.

2. Biologically inspired walking machines

To demonstrate the reactive behavior and to experiment with the neurocontroller of a physical agent, the specific agent's body must be carefully designed because it will define the kind of interactions occurring with its environment. In addition, the body of the agent will also determine the boundary conditions of an environment in which it can operate successfully. The design of the neural control will depend on the morphology of the agent; i.e. the type and position of the sensors and the configurations of the actuators. Choosing too simple a design, the behavior of the body may be of limited interest and it may

1. In this context, the complexity of an agent is determined by the number of degrees of freedom.

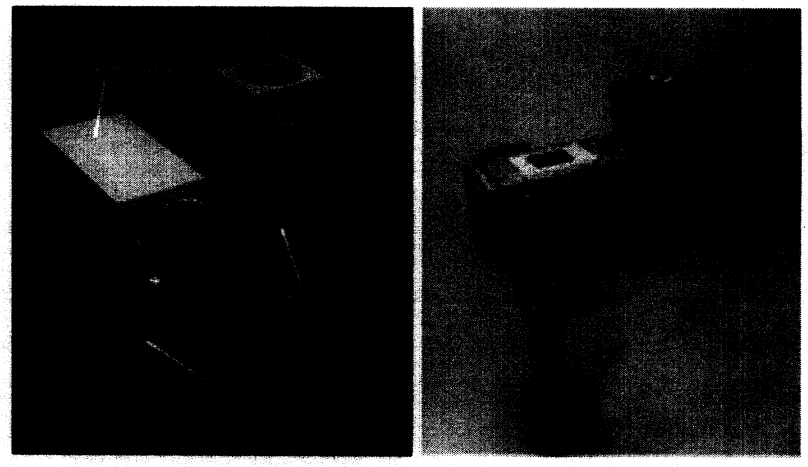

Fig. 2. Leg of the walking machine with two DOF. Left: The 3D model of the leg. Right: The physical leg of the AMOS-WD02.

obstruct the need for an effective neural control for a complex system. To achieve this potential, agents having morphologies similar to walking animals are preferred. In other words, biologically inspired walking machines are the robot platforms for the approach to this work. Moreover, such machines are more attractive because they can behave somewhat like animals and they are still a challenge for locomotion control.

Much research from the domain of biologically inspired walking machines has been done over the last decade. There are several examples of four- and six-legged walking machines. Most of these were designed to have a trunk without a backbone joint, such as *Sprawlita* (Clark et al. 2001), *Tarry I, II* (Frik et al.1999), *LAURON series robots* (Gassmann et al. 2001; *ARAMIES* (Hilljegerdes et al. 2005), *TITAN series robots* (Kato and Hirose 2001), *AirBug* (Kerscher et al. 2002), *Cockroach series robots* (Quinn et al. 2001), *Scorpion* (Spenneberg and Kirchner 2002). However, a few walking machines gain benefits from configurations which promote stability and flexibility of locomotion while maintaining animal characteristics: *BISAM* (Berns et al. 1998), *Robo-Salamander* (Breithaupt et al. 2002), *MechaRoach II* (Wei et al. 2004), *Hyperion* (Yoneda et al. 2001).

Here, the four- and six-legged walking machines are constructed with morphologies analogous to those of salamander and cockroach, respectively. Their structures were initially designed and visualized in 3D models before assembling the physical components. Furthermore, a physical simulation of the walking machines was used to experiment and test their behavior generated by the neurocontroller before downloading it to the physical walking machines.

2.1. The Four-legged Walking Machine AMOS-WD[2]02

The AMOS-WD02 consists of four identical legs where each leg has two joints (two degrees of freedom (DOF)) which are a minimum requirement to obtain the locomotion of a walking machine and which follow the basic principle of movement of a salamander leg. The upper joint of the legs, called the thoracic joint, can move the leg forward (protraction) and backward (retraction) and the lower one, called the basal joint, can move it up (elevation) and down (depression) (Ayers et al. 2000) (compare also Figure 4). The length of the levers which are attached to the basal joints is proportional to the dimension of the machine. They are kept short to avoid greater torque in the actuators. The configuration of the leg built from a construction kit[3] is shown in Figure 2.

Inspired by vertebrate morphology of the salamander's trunk and its motion (Ijspeert 2001) (see also Figure 3), the robot was constructed with a backbone joint which can rotate around a vertical axis. This facilitates a more flexible and faster motion[4]. The backbone joint is also used to connect the trunk, where two hind legs are attached, with the front part where two forelegs are installed.

The trunk and the front part are formed with maximum symmetry to obtain stability of the machine when walking. They are also designed to be as narrow as possible to ensure optimal torque from the supporting legs to the center line of the

2. Advanced MObility Sensor driven-Walking Device.
3. http://www.ais.fraunhofer.de/~breitha/projects/RoboKit/RoboKit.html.
4. Walking speed is approximately 12.7 cm/s when the backbone joint is inactivated while it is approximately 16.3 cm/s with activation of the backbone joint in accordance with the walking pattern (see extension 2). The measurements were done with the walking frequency of the machine at 0.8 Hz.

Fig. 3. Locomotion of a salamander (see from left to right). The open circle in each photo denotes a backbone joint which connects the first segment (1) with the second segment (2) and enables active bending movement of the trunk for locomotion (courtesy of J.S. Kauer (Kauer Lab at Tufts University)).

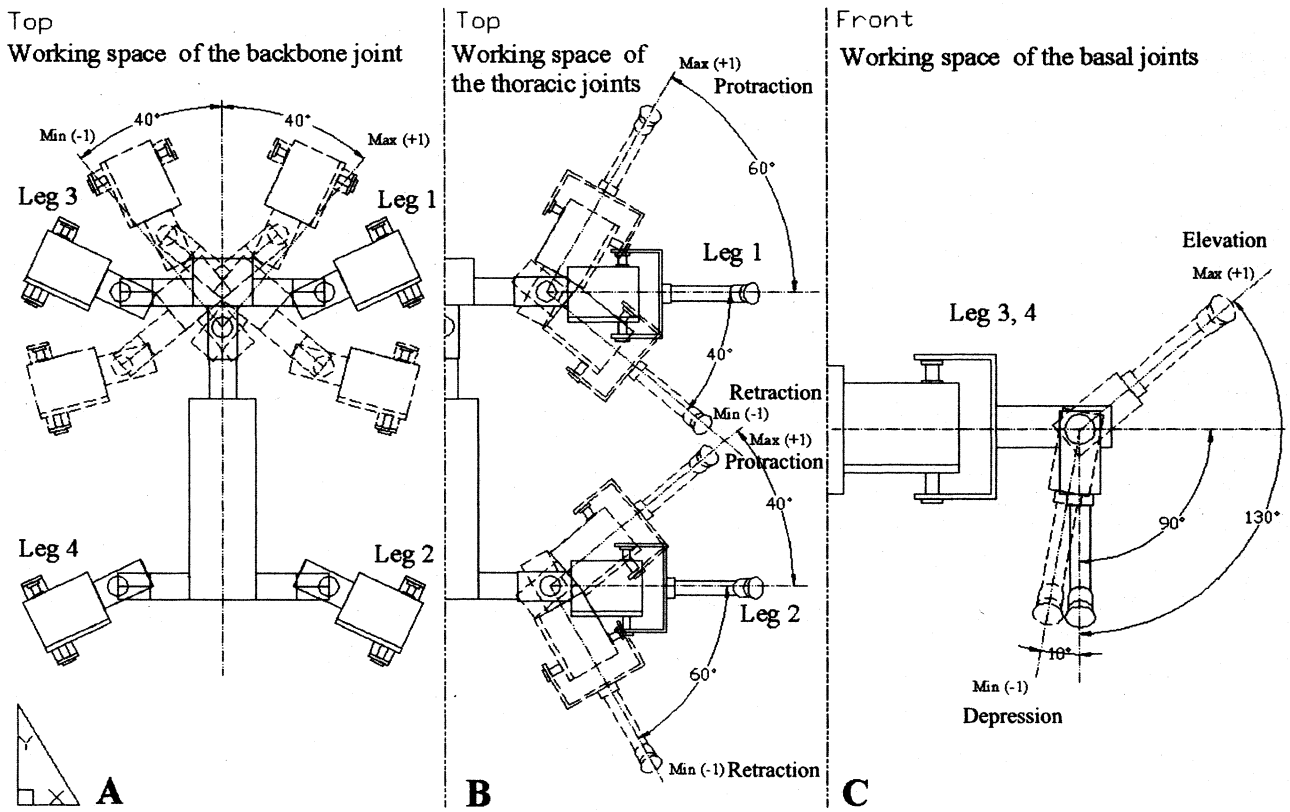

Fig. 4. (A) The angle range of the backbone joint (top view). (B) The angle ranges of all thoracic joints of the right side of the walking machine with the left side being symmetric (top view). (C) The angle range of the basal joint of the left foreleg with the remaining legs having the same angle ranges (front view).

trunk. The construction of the walking machine together with the working space of the legs and the active backbone joint is shown in Figure 4.

A tail with two DOF rotating in horizontal and vertical axes was implemented on the back of the trunk. In fact, this actively moveable tail, which can be manually controlled, is used only

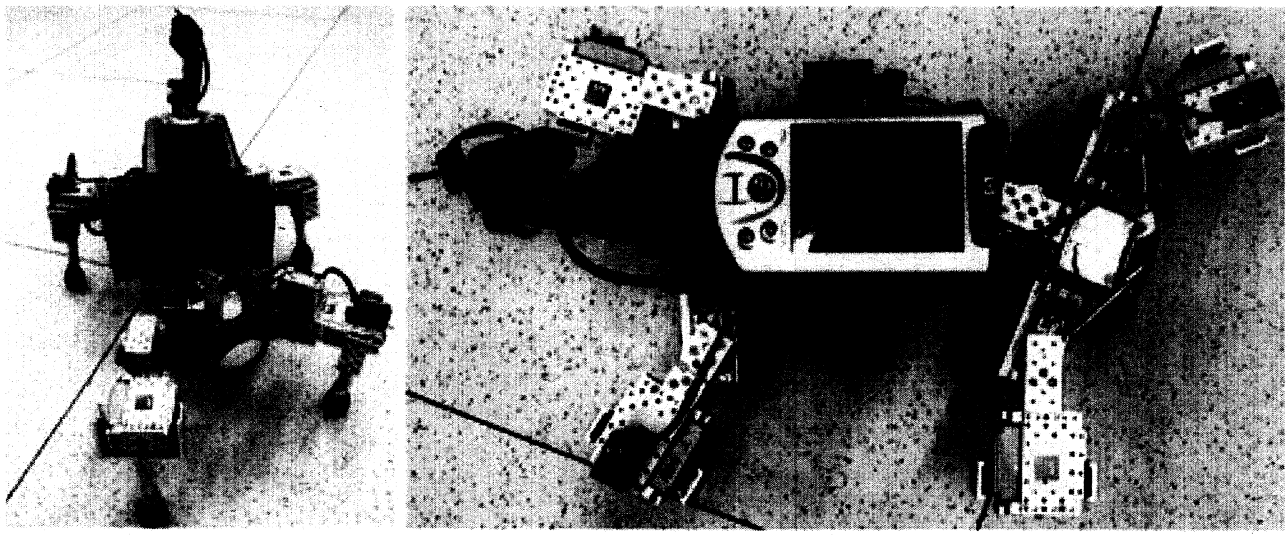

Fig. 5. The four-legged walking machine AMOS-WD02.

to install a mini wireless camera to monitor the environment while the machine is walking. However, the tail also gives the walking machine a more animal-like appearance, e.g. in analogy to a scorpion's tail with a sting (Abushama 1964).

All leg joints are driven by analog servomotors producing a torque between 70 and 90 N cm. The backbone joint is driven by a digital servomotor with a torque between 200 and 220 N cm. For the tail joints, micro-analog servomotors with a torque around 20 N cm were selected. The height of the walking machine is 14 cm without its tail and the weight of the fully equipped machine (including 11 servomotors, all electronic components, battery packs and a mobile processor) is approximately 3.3 kg.

In addition, this machine has two infra-red (IR) sensors installed on the (moveable) front part. They can physically detect obstacles at a distance between 10 and 80 cm. Due to the structure of the four-legged walking machine, its front part, where the sensors were implemented, can turn vertically left and right with respect to the walking pattern by activating the backbone joint. Consequently, the sensors can also scan obstacles over a wide angle. In other words, they perform as an active antenna scanning obstacles in two-dimensional space. The walking machine was also equipped with two mini-microphone sensors to perform sound tropism; these sensors were not used for the experiment described in this article. The physical walking machine is shown in Figure 5.

All in all the AMOS-WD02 has 11 active DOF, four sensors and one wireless camera; therefore, it can serve as a reasonably complex platform for experiments concerning the function of the neural perception-action systems. However, to test the neurocontroller and to observe the resulting behavior of the walking machine (e.g. obstacle avoidance), a physical simulation environment called "YARS" (Yet Another Robot Simulator)[5] is used. The simulator is based on the Open Dynamics Engine (ODE) (Smith 2004). It provides a defined set of geometries, joints, motors and sensors which is adequate to create the walking machine together with its IR sensors in an environment with obstacles (see Figure 6).

YARS enables an implementation which is faster than real time and which is precise enough to reproduce the behavior of the physical walking machine. The simulation environment is connected with the Integrated Structure Evolution Environment (ISEE) (Hülse et al. 2004) which is a software package for the development of neurocontrollers. Finally, after the test on the simulator, the neurocontroller is then downloaded to a mobile processor (a personal digital assistant (PDA)) and the behavior of the machine can be demonstrated in the physical environment. The controller runs with an update frequency of up to 75 Hz. The PDA is interfaced with the multi-servo IO-board[6] (MBoard) which digitizes sensory input signals and generates a pulse width modulated (PWM) signal at a period of 20 ms (50 Hz) to command the servomotors. The communication between the PDA and the MBoard is accomplished via an RS232 interface at 57.6 kbits per second.

5. http://www.ais.fraunhofer.de/INDY/, menu item TOOLS.
6. http://www.ais.fraunhofer.de/BE/volksbot/mboard.htm.

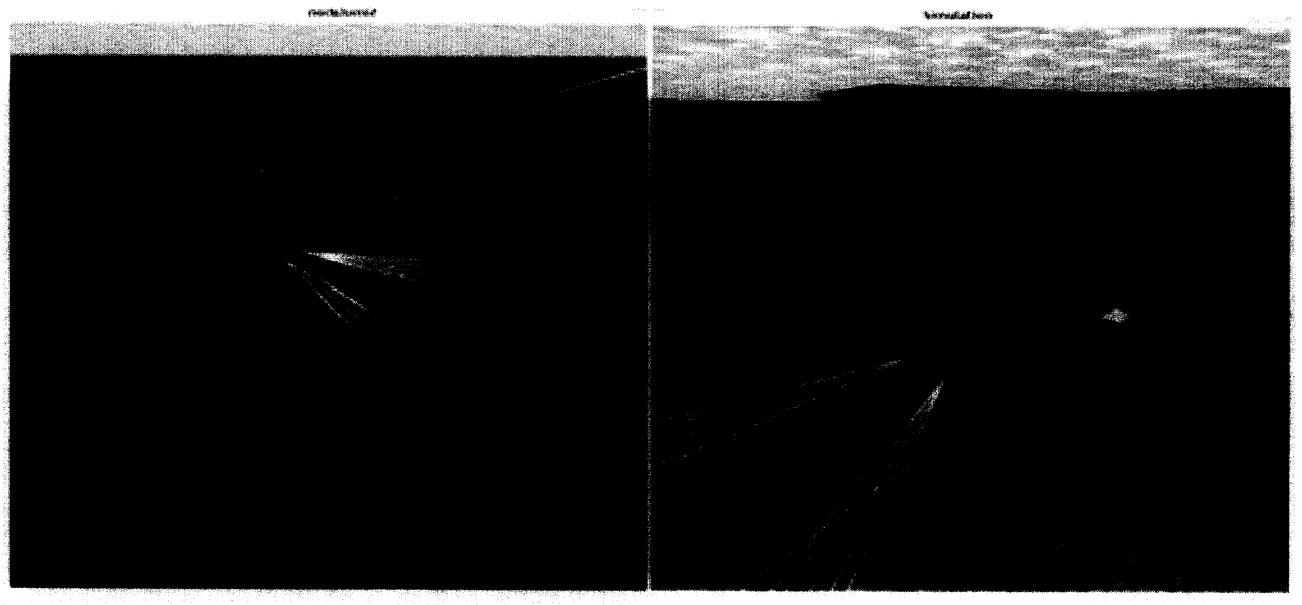

Fig. 6. Different views of the simulated walking machine in its environment. The properties of all simulated components are defined with respect to the physical properties of the walking machine, e.g. weight, dimensions, motor torque, IR sensor and so on.

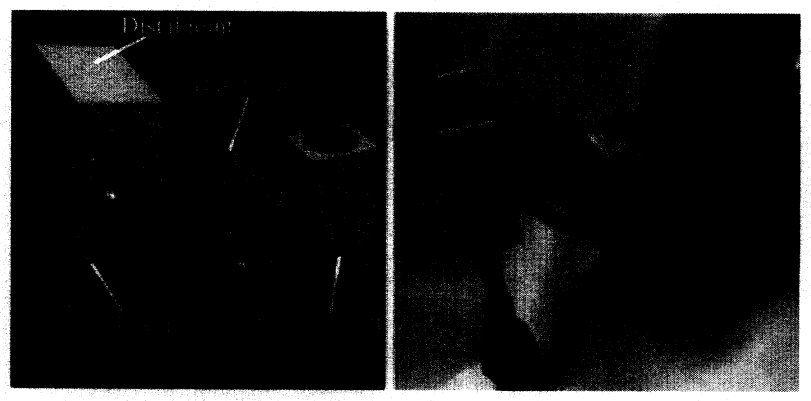

Fig. 7. Leg with three DOF. Left: The 3D model of the leg. Right: The Physical leg of the AMOS-WD06.

2.2. The Six-legged Walking Machine AMOS-WD06

The second walking machine, AMOS-WD06, consists of six identical legs, each with three joints (3 DOF), which is somewhat similar to a cockroach leg (Ritzmann et al. 2004). The thoracic joint has similar functionality to the thoracic joint of the AMOS-WD02, while the other two joints, the basal and distal joints, are used for lifting (elevation) and lowering (depression) and for extension and flexion of the leg (Ayers et al. 2000). The levers which are attached to distal joints were built in the same manner as the levers of the AMOS-WD02. The configuration of the leg is shown in Figure 7.

This leg configuration provides the machine with the possibility to perform omnidirectional walking; i.e. the machine can walk forwards, backwards, laterally and can turn with different radii. Additionally, the machine can also perform a diagonal forward or backward motion to the left or the right by activating the forward or backward motion together with the lateral left or right motion. The high mobility of the legs enables the walking machine to walk over an obstacle, stand in an upside-

Fig. 8. Left: The AMOS-WD06 walks over an obstacle of maximum height 7 cm; Middle: stands in an upside-down position; and Right: climbing position on obstacles, which is enabled by the active backbone joint.

Fig. 9. A cockroach climbs over large obstacles. It can bend its trunk downward at the joint between the first (T1) and second (T2) thoracic to keep the legs close to the top surface of the obstacles for an optimum climbing position and even to prevent unstable actions (modified from Ritzmann et al. (2004) with permission).

down position (see extension 2) and even climb over obstacles[7] (see Figure 8).

Inspired by the invertebrate morphology of the American cockroach's trunk and its motion (see Figure 9), a backbone joint which can rotate in a horizontal axis was constructed. It imitates a connection between the first (T1) and second (T2) thoracic of a cockroach. Thus, it will provide enough mobility for the machine to climb over an obstacle by lifting the front legs up to reach the top of an obstacle and then bending them downward during step climbing (compare Figures 8 right and 10C).

However, this active backbone joint will be fixed under normal walking conditions of the machine. It is mainly used to connect the trunk (second thoracic), where two middle legs and two hind legs are attached, with the front part (first thoracic), where two forelegs are installed. The trunk and the front part were designed using the same concept as for the AMOS-WD02. An active tail, similar to that of the AMOS-WD02, was also implemented on the back of the trunk. It is used for the same purpose as the AMOS-WD02's tail described above. The construction of the AMOS-WD06 together with the working space of the legs and the active backbone joint is shown in Figure 10.

All leg joints are driven by analog servomotors producing a torque between 80 and 100 N cm. For the backbone joint and the tail joints, the same motors which were used on the AMOS-WD02 were employed. The height of the walking machine is 12 cm without its tail and the weight of the fully equipped robot (including 21 servomotors, all electronic components, battery packs and a mobile processor) is approximately 4.2 kg.

7. Note that the controller driving the machine fitted with the backbone joint is not described in this paper; it will be published elsewhere together with the technical details for climbing.

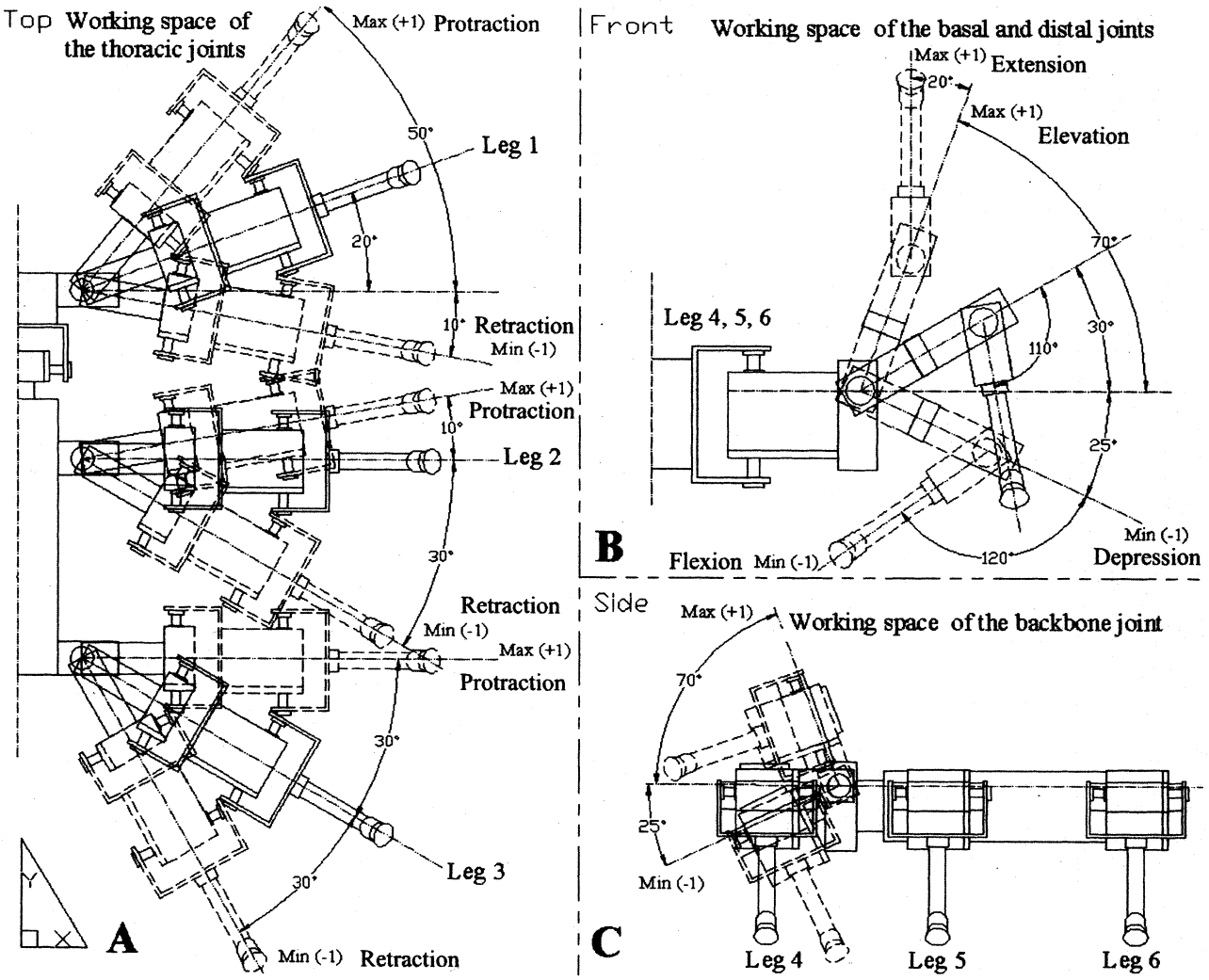

Fig. 10. (A) The angle ranges of all thoracic joints on the right side of the walking machine, with the left side being symmetric (top view). (B) The angle ranges of the basal and distal joints of the left foreleg with the remaining legs having the same angle ranges (front view). (C) The angle range of the backbone joint (side view).

Like the AMOS-WD02, a mini wireless camera with a built-in microphone was also installed on the tail. In addition, the walking machine has one upside-down detector which is attached at the side of the trunk of the machine, and six IR sensors to detect obstacles. Two of them, which can physically detect obstacles at long distance between 20 and 150 cm, were fixed to the front part while the rest of them, operating at a shorter distance between 4 and 30 cm, were fixed at the levers of the two front and two middle legs. They help prevent the walking machine legs from hitting obstacles, like the legs of chairs or desks.

All in all the AMOS-WD06 has 21 active degrees of freedom, seven sensors and one wireless camera; thus it can also serve as a test platform like the AMOS-WD02. The AMOS-WD06 was also simulated by the YARS with the same environment and the same purpose as described above. The basic features of the simulated walking machine are close to those of the physical walking machine, e.g. weight, dimension, motor torque and so on. It consists of body parts (front part, backbone joint, trunk and limbs), servomotors, IR sensors and an additional tail. The simulated walking machine with its environment is shown in Figure 11.

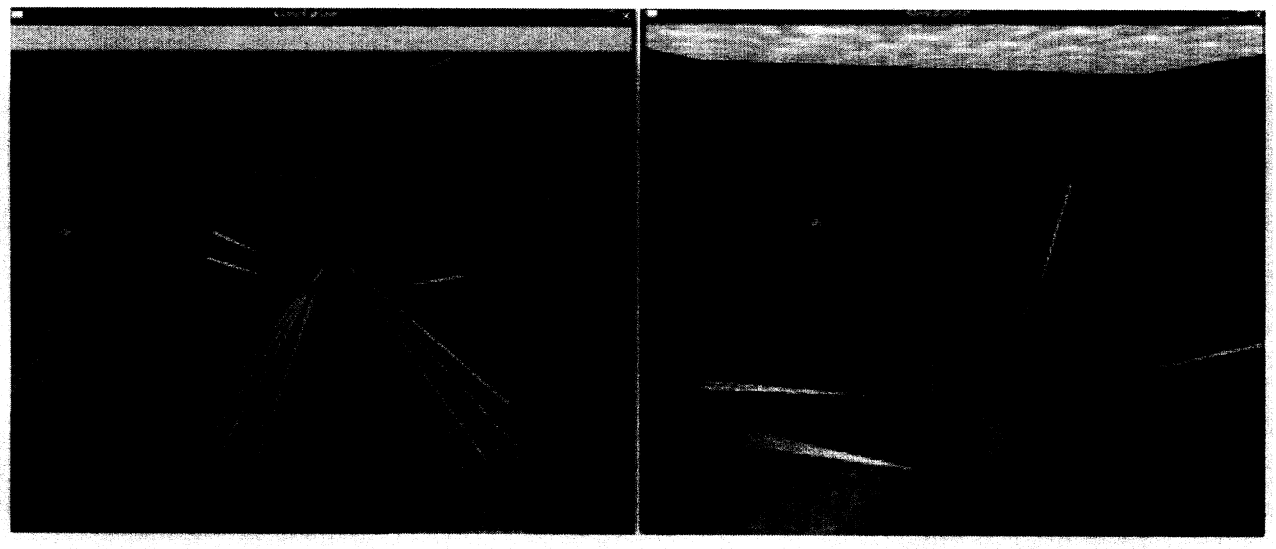

Fig. 11. Different views of the simulated walking machine in its environment.

The final neurocontroller will also be implemented on the physical walking machine to test its behavior in a physical environment. Again, the neurocontroller is programmed on the same mobile processor system with the same update frequency as the AMOS-WD02.

3. Artificial Neural Perception-Action System

In order to create a robust and effective neurocontroller which is able to generate exploration and obstacle-avoidance behaviors of physical machines, the dynamic properties of recurrent neural networks are utilized. The standard additive neuron model with sigmoidal transfer function together with its discrete-time dynamics is given by

$$a_i(t+1) = \sum_{j=1}^{n} W_{ij} \tanh(a_j(t)) + B_i \quad i = 1, \ldots, n \qquad (1)$$

where n denotes the number of units, a_i their activity, B_i represents a fixed internal bias term together with a stationary input to neuron i, and W_{ij} the synaptic strength of the connection from neuron j to neuron i. The output o_i of the neuron is given by the sigmoidal transfer function $tanh$, i.e. $o_i = tanh(a_i)$. Input units are configured as linear buffers. The modular neurocontroller for the desired behavior is described in detail in the following sections.

3.1. Neural Preprocessing Network

To obtain obstacle avoidance behavior driven by signals from the IR sensors, preprocessing of the sensor signal is required. Here, the property of the minimal recurrent controller (MRC) (Hülse and Pasemann 2002) is applied. The MRC has been developed to control the two-wheel miniature Khepera robot (Mondada et al. 1993). The preprocessing network was developed and analyzed using the physical simulation environment (YARS) connected to the ISEE. The simulation was implemented on a 1 GHz PC with an update frequency of 75 Hz.

On the basis of its well understood functionality (Hülse and Pasemann 2002) the parameters were manually readjusted with the help of the simulation. First, the weights from the input to the output units were set to a high value to amplify the sensory signals, i.e. 7. As a result, under some conditions the sensory noise was eliminated. In fact, these high multiplicative weights drive the output signals to switch between two saturation values, one low (≈ -1) and the other high ($\approx +1$). Then the self-connection weights of the output neurons were manually adjusted to derive a reasonable hysteresis interval on the input space. The width of the hysteresis is proportional to the strength of the self-connection. This effect determines the turning angle in front of obstacles when avoiding obstacles, i.e. the greater the hysteresis, the larger the turning angle. Both self-connections are set to 5.4 to obtain a suitable turning angle of the four-legged walking machine. Finally, the recurrent connections between output neurons were symmetrized and manually adjusted to the value -3.55. This guarantees optimal functionality for avoiding obstacles and escaping from sharp corner situations. The resulting network is shown in Figure 12.

Generally, this preprocessing network together with the two IR sensors installed on the front part of the walking machine is sufficient to sense obstacles on the left and right front. How-

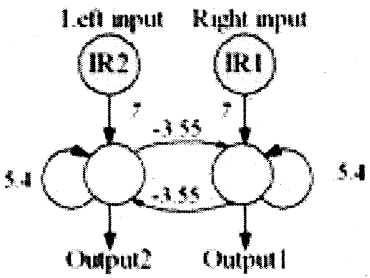

Fig. 12. Neural preprocessing network for two sensory inputs with appropriate weights. The network is developed to operate with an update frequency of 75 Hz. Here, it is applied to control the AMOS-WD02.

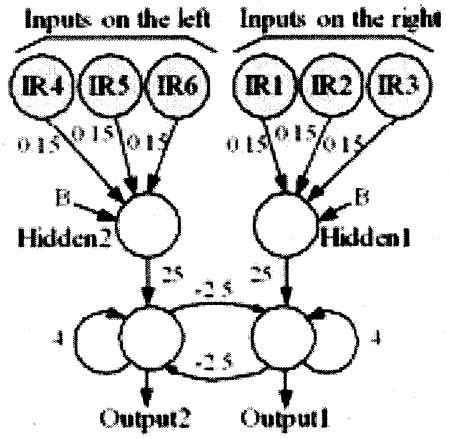

Fig. 13. Neural preprocessing network for six sensory inputs with appropriate weights. The network is also developed to operate at an update frequency of 75 Hz. Here, it is applied to control the AMOS-WD06.

ever, to enhance the avoiding capacity, e.g. protecting the legs of the walking machine from hitting obstacles, such as the legs of chairs or desks, one can easily install more sensors on the levers of the legs, and send their signals to the corresponding input neurons of the network.

For instance, by implementing six sensors on the AMOS-WD06, the three sensory signals on each side are simply connected with hidden neurons which are directly connected with the two original output neurons with large weights (see Figure 13). To stay in the linear domain of the sigmoidal transfer function of the hidden neuron, each sensor signal is multiplied by a small weight, here 0.15, and the bias term B is set to determine a threshold value of the sum of the input signals, e.g. 0.2. When the measured value is greater than the threshold in any of the three sensory signals, excitation of the hidden neuron on the corresponding side occurs. Consequently, the activation of each hidden neuron can vary in the range between ≈ -0.245 ("no obstacle is detected") and ≈ 0.572 ("all three sensors on the appropriate side simultaneously detect obstacles"). And, the weights from the hidden to the output units are set to a high value, e.g. 25, to amplify these signals. Again, the other parameters (self-connection and recurrent-connection weights of the output neurons) were manually optimized in a similar way to that described above. As a result, they are set to 4 and -2.5, respectively. The improved structure of this neural preprocessing network together with its optimized weights is shown in Figure 13.

In both cases (see Figures 12 and 13), all sensory signals are linearly mapped onto the interval $[-1, +1]$ before feeding into the networks, with -1 representing "no obstacles", and $+1$ "a near obstacle is detected". Subsequently, the final output signals of the network (*Output*1, *Output*2) will be directly connected to other networks, called the VRNs, described later. The parameters of both networks are set in such a way that the noise of the sensory signals is eliminated. This is due to the hysteresis effect generated by the "super-critical" self-connections (> 1) of the output neurons (Hülse and Pasemann 2002). The network shown in Figure 13 is selected to illustrate the hysteresis effect and its capability to filter the sensory noise (see Figure 14).

In addition, there is a third hysteresis phenomenon involved which is associated with the *even loop* of the inhibitory connection (Pasemann 1993) between the two output neurons. Under general conditions, only one neuron at a time is able to have a positive output, while the other one has a negative output, and vice versa. The network shown in Figure 13 is again used to demonstrate this phenomenon (see Figure 15).

This phenomenon is responsible for the escape from sharp corners as well as from deadlock situations. Finally, *Output*1 and *Output*2 of the neural preprocessing network together with the VRNs, described below, determine the behavior of the walking machines; especially, the switching between different walking modes, as from "walking forwards" to "turning left" when there are obstacles on the right. The network outputs also control turning direction of the walking machines in corners or deadlock situations depending on which sensor side has previously been active (compare Figure 15). In special situations, like walking towards a wall, sensors on both sides might give positive outputs at the same time, and, because of the VRNs, the walking machines will walk backwards. During walking backwards, the activation of the sensory signal of one side might still be active while the other might be inactive. Correspondingly, the walking machines will turn into the direction opposite to that of the active signal, and finally leave the wall.

3.2. Neural Oscillator Network

The concept of neural oscillators for walking machines has often been studied (Billard and Ijspeert 2000; Endo et al. 2005;

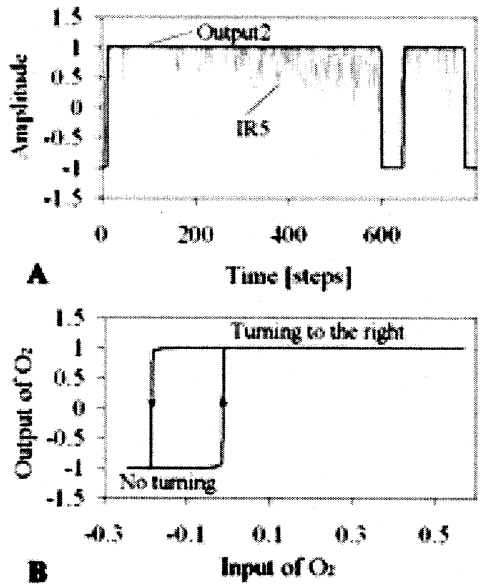

Fig. 14. (A) Sensory signal ($IR5$, gray line) before preprocessing and the output signal 2 ($Output2$, solid line) after preprocessing. (B) The "hysteresis effect" for the output signals of neuron 2 (O_2). The input signal of O_2 varies between ≈ -0.245 and ≈ 0.572 back and forth while the input of the output neuron 1 (O_1) is set to ≈ -0.245 ("no obstacles are on the right side"). When the output of O_2 is active (≈ 1); i.e. "obstacles are on the left side", then the walking machine will turn right until the output becomes inactivated (≈ -1). On the other hand, if such a condition occurs for O_1, the input of O_1 will show the same hysteresis effect as the input of O_2 does.

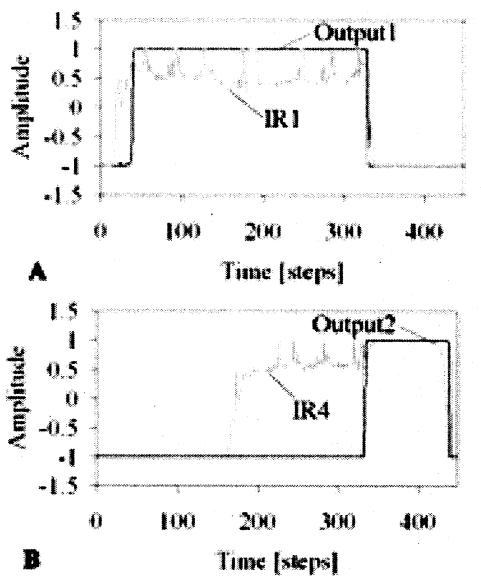

Fig. 15. (A) and (B) present the sensory signals ($IR1$ and $IR4$, gray line) and the output signals ($Output1$ and $Output2$, solid line), respectively. Due to the inhibitory synapses between two output neurons and the high activity of O_1 (A), $Output2$ (B) is still inactive although $IR4$ becomes activated at around 170 time steps. At around 320 time steps, the switching condition between $Output1$ and $Output2$ occurs because $IR1$ becomes inactivated, meaning "no obstacles detected" while $IR4$ is still active, meaning "obstacles detected".

Lewis et al. 2005; Nakada et al. 2003; Taga et al. 1991). For instance, Kimura and Fukuoka (2004) constructed a neural oscillator network with four neurons. The network was applied to control the four-legged walking machine $TEKKEN$ where each hip joint of the machine is driven by one of the neurons. Ayers (2002) used a neural oscillator consisting of so-called elevator and depressor synergies. They are arranged as an endogenous pacemaker network with reciprocal inhibition, and are used to generate walking patterns for the 8-legged *Lobster* robot.

Here, a so-called "SO(2)-network" (Pasemann et al. 2003) is employed. It is used as a central pattern generator (CPG) (Ayers et al. 2000; Kirchner et al. 2002; Markelic 2005; Righetti and Ijspeert 2006) which follows one principle of locomotion control of walking animals (Cruse 2002; Hooper 2000; Marder and Calabrese 1996; Stein et al. 1997). It generates the rhythmic movement for basic locomotion of the walking machines without the requirement for sensory feedback. The network structure is shown in Figure 16.

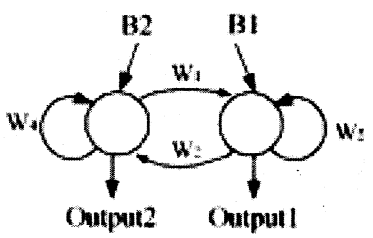

Fig. 16. Structure of the 2-neuron network.

Its parameters are experimentally adjusted using the ISEE to acquire the optimal oscillating output signals for generating locomotion of the walking machines. The parameter set is selected with respect to the dynamics of the 2-neuron system, staying near the Neimark–Sacker bifurcation where the quasi-periodic attractors occur (Pasemann et al. 2003). Examples of different oscillating output signals generated by different weights and bias terms are presented in Figure 17.

Figure 17 shows that such a network has the capability to generate various oscillating outputs depending on the weights

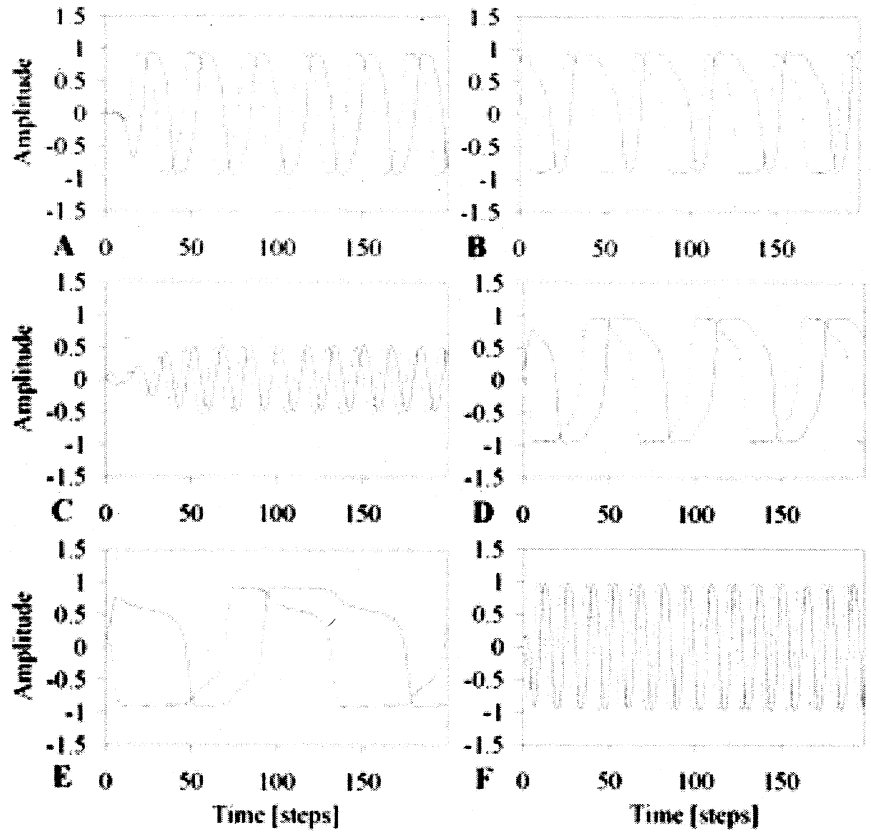

Fig. 17. Oscillating output signals of neurons 1 (dashed line) and 2 (solid line) from the network having different weights and bias terms. The resulting output signals for (A) small bias terms ($B_1 = B_2 = 0.0001$) while $W_1 = -0.4$, $W_2 = 0.4$ and $W_3 = W_4 = 1.5$, and (B) for larger bias terms ($B_1 = B_2 = 0.1$) and all weights as in (A). (C) For smaller self-connection weights ($W_3 = W_4 = 1$) with $W_1 = -0.4$, $W_2 = 0.4$ and bias terms = 0.01. (D) For larger self-connection weights ($W_3 = W_4 = 1.7$) and all weights together with bias terms as in (C). (E) For smaller absolute values of connection weights between two output neurons ($W_1 = -0.25$, $W_2 = 0.25$) with $W_3 = W_4 = 1.5$ and the bias terms = 0.01. (F) For larger absolute values of connection weights between two output neurons ($W_1 = -0.8$, $W_2 = 0.8$) and all weights together with bias terms as in (E).

and the bias terms. For instance, if the bias terms are small (compare Figure 17A), the initial output signals will oscillate with a very small amplitude and then the amplitude will increase during a transient time, while the amplitude of the output signals for large bias terms is high right from the beginning (compare Figure 17B). Furthermore, different bias terms also affect the waveform of the output signals. Different self-connection weights result in different amplitudes and waveforms of the oscillating output signals (compare Figures 17C and D). To adjust the oscillating frequency of the outputs, one can also control the connection weights between two output neurons; i.e. for small connection weights (absolute values), the output signals oscillate at low frequency while large connection weights (absolute values) make the outputs oscillate at high frequency with different waveforms (compare Figures 17E and F).

However, one can utilize such a modifiable oscillating output behavior with respect to the weights and the bias terms in the field of neural control, e.g. to control the type of walking and the walking speed of legged robots (Fischer et al. 2004; Markelic 2005). Here, the actual parameter set for the network controller is $B_1 = B_2 = 0.01$, $W_1 = -0.4$, $W_2 = 0.4$ and $W_3 = W_4 = 1.5$, where the sinusoidal outputs correspond to a quasi-periodic attractor (see Figure 18).

The output of neuron 1 ($Output1$) is used to drive all thoracic joints and an additional backbone joint, and the output

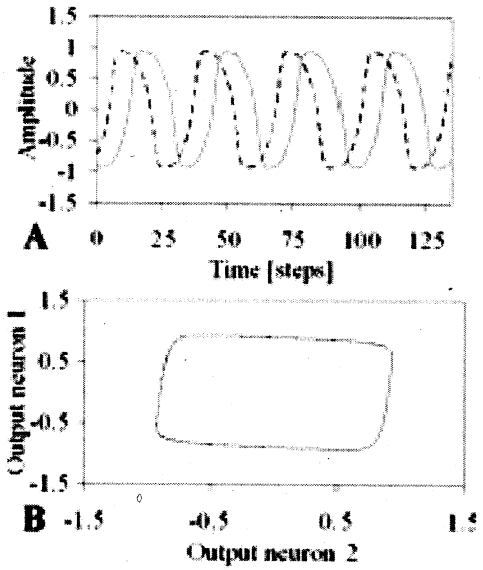

Fig. 18. (A) Output signals of neurons 1 (dashed line) and 2 (solid line) from the neural oscillator network. (B) Phase space with quasi-periodic attractor of the oscillator network, which is used to drive the legs of the machines.

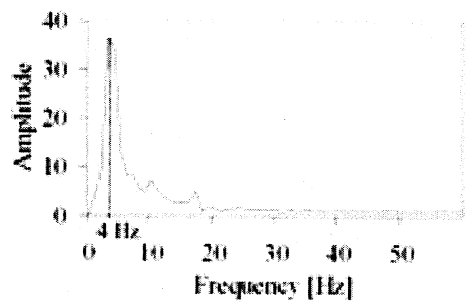

Fig. 19. Fast Fourier Transform (FFT) spectrum of the sinusoidal output recorded for 5 s shows that it has an eigenfrequency around 4 Hz. Then, the walking frequency of the machines can be approximately (4/5) 0.8 Hz.

of neuron 2 (*Output*2) is used to drive all basal joints (and all distal joints for 3-DOF legs). This neural oscillator network is implemented on the PDA with an update frequency of 25.6 Hz. It generates a sinusoidal output with a frequency of approximately 0.8 Hz (see Figure 19) analyzed by the free scientific software package Scilab-3.06[8].

By using asymmetric connections from the oscillator outputs to corresponding motor neurons (compare Figures 24 and 25), a typical trot gait for a four-legged walking machine and a typical tripod gait for a six-legged walking machine are obtained, which are similar to the gaits of a cat and a cockroach, respectively. In a trot gait as well as a tripod gait, the diagonal legs are paired and move together. These typical gaits will enable efficient forward motions.

3.3. *Velocity Regulating Network*

To change the walking mode, e.g. from walking forwards to walking backwards and from turning left to turning right, the efficient way is to perform a 180 degree phase shift of the sinusoidal signals which drive the thoracic joints. To do so, the velocity regulating network (VRN) is introduced (see Figure 21A). The network used is taken from Fischer (2004). It approximates the multiplication function of two input values $x, y \in [-1, 1]$ (compare Figure 20). One can optimize this approximation, for instance by using backpropagation, but for the purposes of controlling the machine, it is good enough. Multiplication by higher-order synapses is not used here for consistency reasons.

For this purpose the input x is the oscillating signal (*Output*1) from the neural oscillator network used to generate the locomotion and the input y is the preprocessed sensory signal from the neural preprocessor used to drive the corresponding behavior. Figure 21A presents the VRN, consisting of four hidden neurons and one output neuron. Figure 21B shows that the output signal is subject to a phase shift of 180 degrees when the sensory signal (input y) changes from -1 to $+1$ and vice versa.

Because the VRN behaves qualitatively like a multiplication function, it should also be able to increase or decrease the amplitude of the oscillating signal. To explore the behavior of this network, a fixed oscillating signal is connected to the input x of the network while the input y has constant input values to be multiplied by the oscillating signal. The resulting outputs for the different y-input values are shown in Figure 22.

From Figure 22, it can be seen that the network is not only able to make a 180 degree phase shift of the oscillatory output signal but, using the y-input, it can also modulate its amplitude. In particular, the amplitude of the output will be 0 if the given y-input is equal to 0. This function of the network enables the machines to perform different modes by making a 180 degree phase shift of the oscillatory signal. It can stop the walking machines by setting the y-input to 0. Furthermore, the different amplitudes of the oscillating signal will affect the walking speed of the machines; i.e. the higher the amplitude of the signal the faster they walk and vice versa.

To compare the effect of the different amplitudes of the oscillating signal with the walking speed of the machines, the VRNs together with the neural oscillator network are implemented on the mobile processor of the AMOS-WD02. The network is updated at 25.6 Hz. To determine the walking speed of the machine depending on the y-input values, the time

8. http://www.scilab.org/.

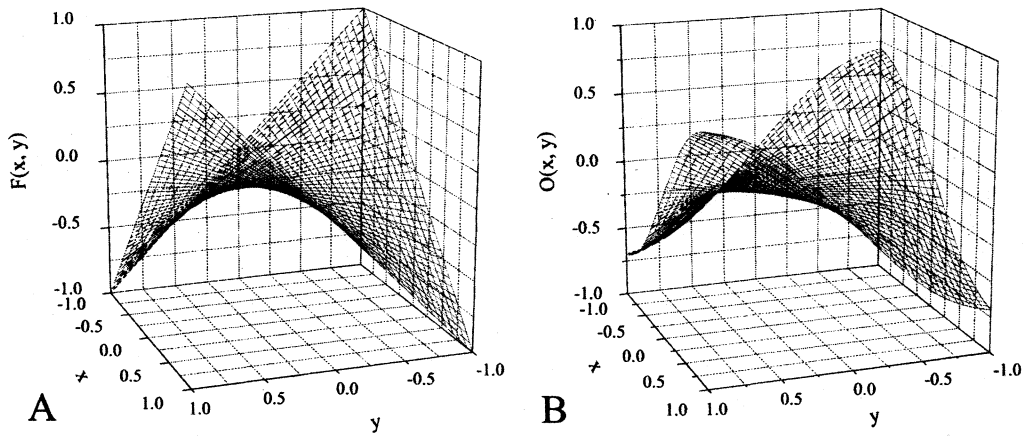

Fig. 20. (A) The multiplication function $F(x, y) = x \cdot y$, and (B) its approximation $O(x, y)$ of the VRN with average mean square error $(e^2) \approx 0.0046748$. The output O of the neuron is given by the sigmoidal transfer function *tanh*; therefore suitable input values x, y are in the range of $[-1 \cdots 1]$.

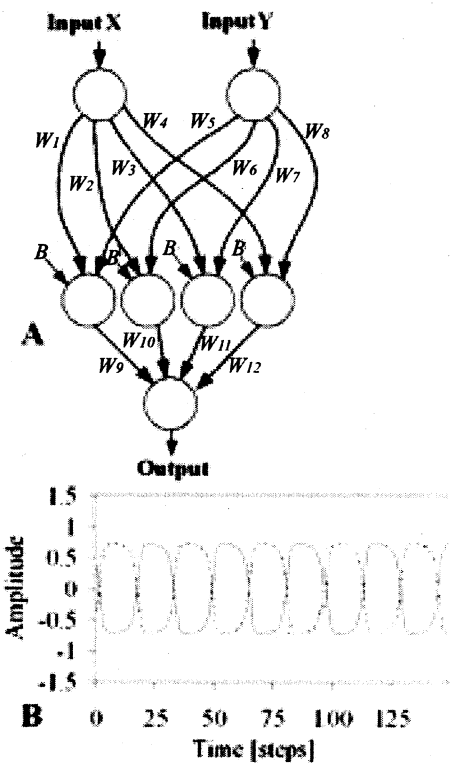

Fig. 21. (A) VRN with four hidden neurons where the parameter set for the network is $W_1 = W_3 = W_5 = W_8 = 1.7246$, $W_2 = W_4 = W_6 = W_7 = -1.7246$, $W_9 = W_{10} = 0.5$, $W_{11} = W_{12} = -0.5$ and the bias terms B are all equal to -2.48285. (B) Output signal for $y = +1$ (solid line), and for $y = -1$ (dashed line).

needed to cover a fixed distance (1 m) was measured several times for every y-input. The average speed values for the different y-input levels are displayed in Figure 23.

As a result, the VRN together with the neural oscillator network can accelerate, decelerate or stop the motion of the walking machines simply driven by the y-input of the VRN.

3.4. Modular Reactive Neurocontroller

The integration of two different functional neural modules, *the neural preprocessing and the neural control (the neural oscillator network and the velocity regulating networks)*, gives the complete modular neurocontroller. This controller is able to generate exploration and reactive obstacle avoidance behaviors. One oscillating output signal from the neural oscillator network is directly connected to all basal joints[9] (and distal joints in case of 3-DOF legs), while the other one is connected to the thoracic joints, only indirectly, passing through the VRNs via their x-inputs (compare Figure 21A).

Here, the output signals of the neural preprocessing network go to *Input*1 (I_1) and *Input*2 (I_2) of the VRNs (compare Figures 24 and 25). Thus, the rhythmic leg movements are generated by the neural oscillator network and the steering is realized by the VRNs in accordance with the outputs of the neural preprocessing module. The structure of this controller

9. Recall that, a basal joint is for elevation and depression, a distal joint is for extension and flexion and a thoracic joint is for protraction and retraction of the leg (see Figures 4 and 10).

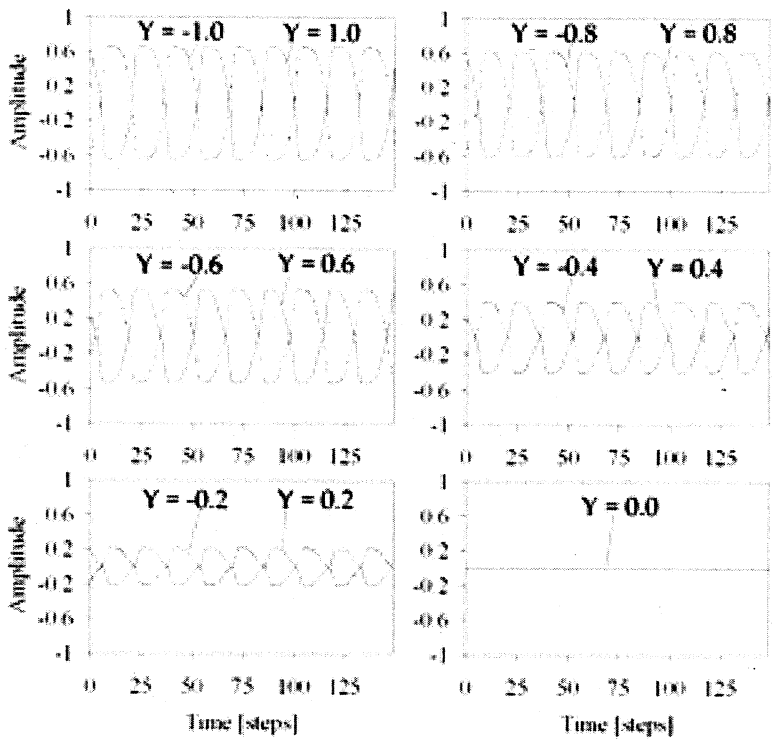

Fig. 22. Output signal (solid line) when the y-input is equal to a positive value and the output signal (dashed line) when the y-input is equal to a negative value. The different given values of the y-input result in the different amplitudes of the output signal.

and the location of the corresponding motor neurons on the four-legged walking machine AMOS-WD02 are shown in Figure 24. The weight matrix of the internal structure is given by

$$\begin{pmatrix}
1.5 & 0.4 & 0 & 0 & 0 & 0 & 0 & 0 & 0 & 0 & 0 & 0 & 0 & 0 \\
-0.4 & 1.5 & 0 & 0 & 0 & 0 & 0 & 0 & 0 & 0 & 0 & 0 & 0 & 0 \\
0 & 0 & 0 & 0 & 0 & 0 & 0 & 0 & 0 & 0 & 0 & 0 & 0 & 0 \\
0 & 0 & 0 & 0 & 0 & 0 & 0 & 0 & 0 & 0 & 0 & 0 & 0 & 0 \\
0 & a & a & 0 & 0 & 0 & 0 & 0 & 0 & 0 & 0 & 0 & 0 & 0 \\
0 & -a & -a & 0 & 0 & 0 & 0 & 0 & 0 & 0 & 0 & 0 & 0 & 0 \\
0 & a & -a & 0 & 0 & 0 & 0 & 0 & 0 & 0 & 0 & 0 & 0 & 0 \\
0 & -a & a & 0 & 0 & 0 & 0 & 0 & 0 & 0 & 0 & 0 & 0 & 0 \\
0 & a & 0 & a & 0 & 0 & 0 & 0 & 0 & 0 & 0 & 0 & 0 & 0 \\
0 & -a & 0 & -a & 0 & 0 & 0 & 0 & 0 & 0 & 0 & 0 & 0 & 0 \\
0 & a & 0 & -a & 0 & 0 & 0 & 0 & 0 & 0 & 0 & 0 & 0 & 0 \\
0 & -a & 0 & a & 0 & 0 & 0 & 0 & 0 & 0 & 0 & 0 & 0 & 0 \\
0 & 0 & 0 & 0 & b & b & -b & -b & 0 & 0 & 0 & 0 & 0 & 0 \\
0 & 0 & 0 & 0 & 0 & 0 & 0 & 0 & b & b & -b & -b & 0 & 0
\end{pmatrix}$$

where elements W_{ij} refer to the synaptic strength of the connection *from* neuron j *to* neuron i (compare Figures 24 and 25). The parameters a and b are set to $a = 1.7246$ and $b = 0.5$.

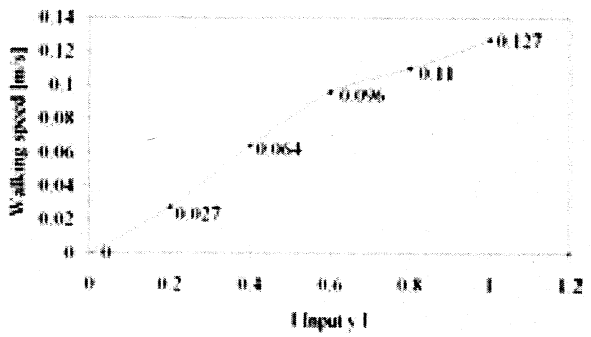

Fig. 23. This shows that |input y| $= 0.2$ generates a small oscillatory amplitude resulting in slow motion (0.027 m/s). On the other hand, |input y| $= 1.0$ causes a high amplitude and fast motion (0.127 m/s).

The controller of the four-legged walking machine can also be applied to control even more complex systems (more degrees of freedom), like the six-legged walking machine AMOS-WD06, without changing the internal parameters or the structure of the networks (compare Figures 24 and 25).

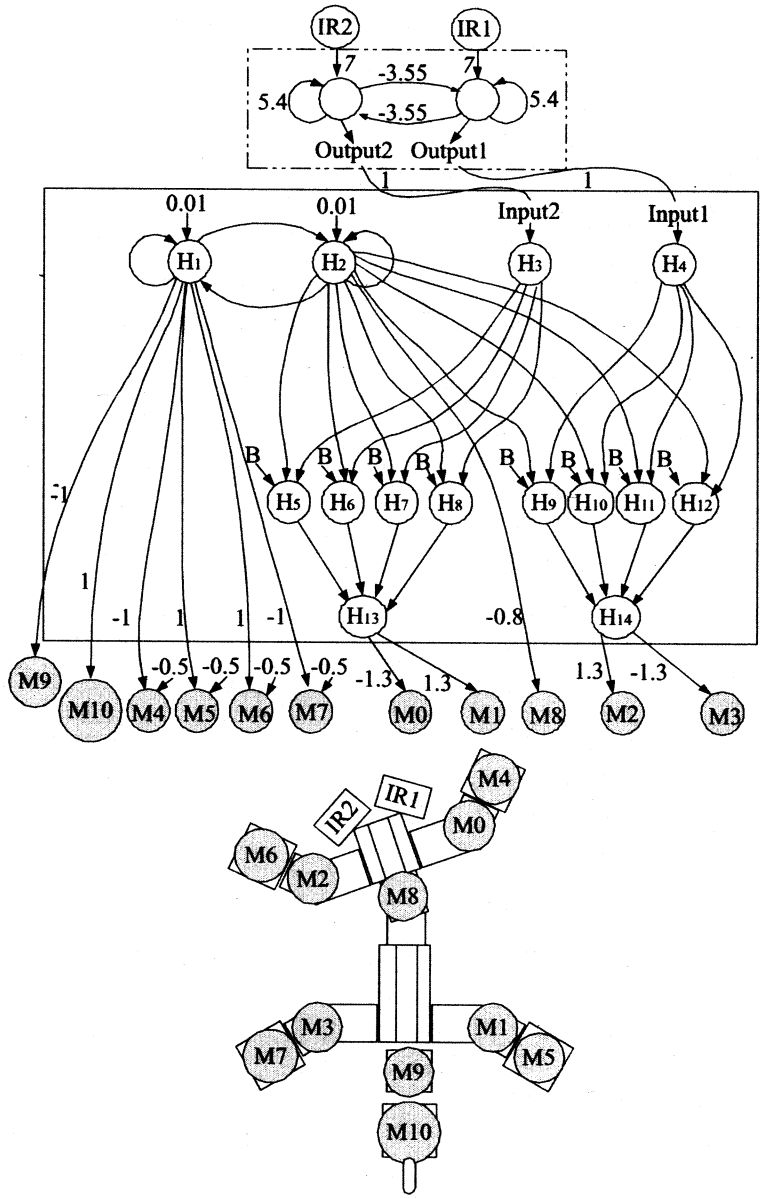

Fig. 24. Modular reactive neurocontroller of the AMOS-WD02 (see right panel in extension 1). It generates a trot gait which is modified when I_1 or I_2 is changed by the sensory signals. The bias terms B of the VRNs are all equal to -2.48285. The outputs from the neural preprocessing module (dashed frame) are directly connected to the input neurons (I_1, I_2) of the neural control module (solid frame). The synaptic strength of the connections of the internal structure (solid frame) can be seen from the weight matrix above.

The network structure and the corresponding positions of the motors of the AMOS-WD06 are shown in Figure 25. And, the weight matrix of its internal structure is the same as described above.

Comparing the controllers of both machines, one can see from Figures 24 and 25 that the internal structure and parameters of the modules (solid frame) are fixed, and only motor and sensor neurons are added. Because the design comprises inde-

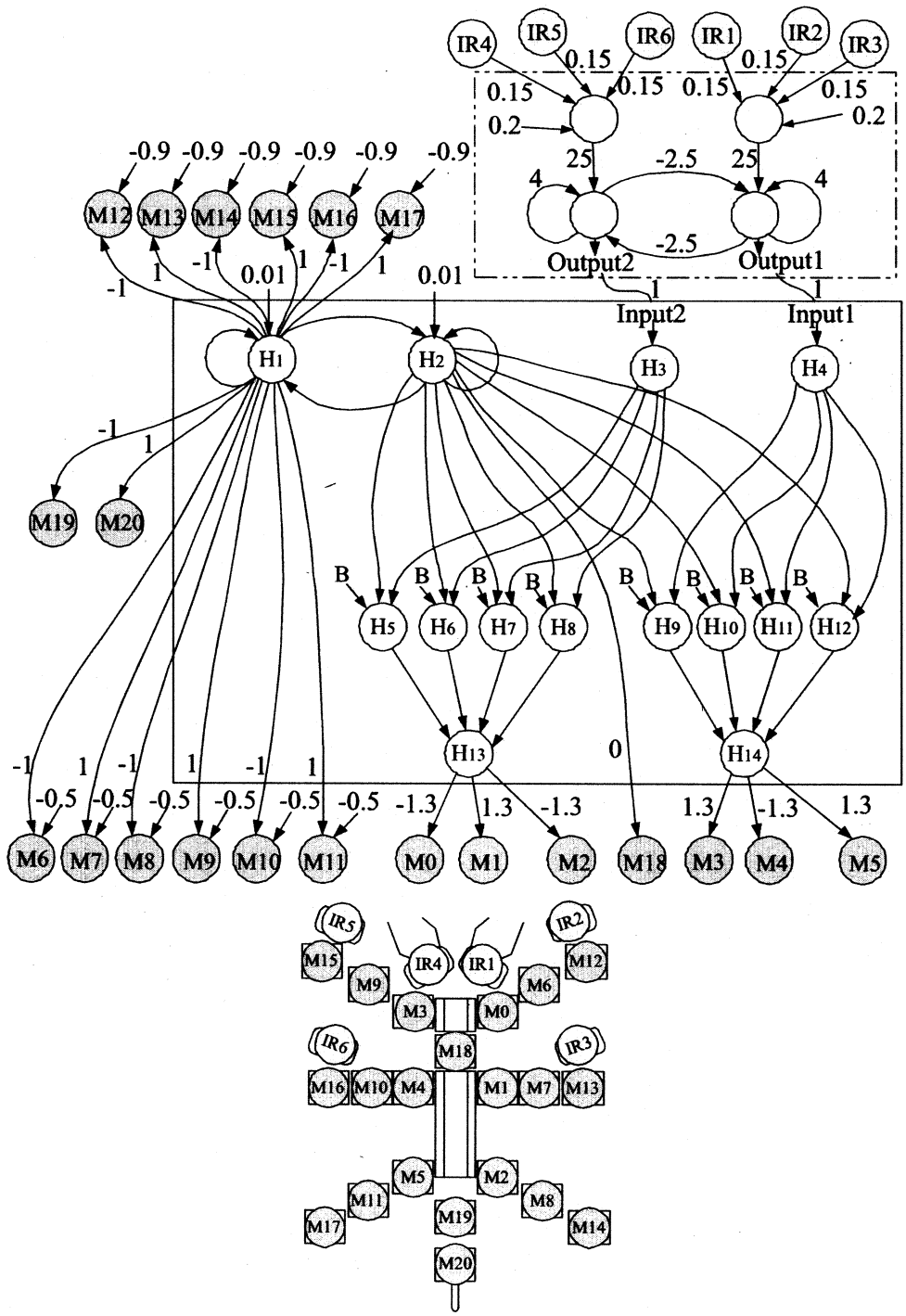

Fig. 25. Modular reactive neurocontroller of the six-legged walking machine AMOS-WD06 (see right panel in extension 1). The bias terms B of the VRNs are again all equal to -2.48285. The synaptic strength of the connections of the internal structure (solid frame) can be seen from the weight matrix above.

pendent modules the neural preprocessing network for the IR sensors (dashed frame in Figures 24 and 25) can be replaced with other types of signal processing modules to obtain different reactive behaviors, e.g. auditory signal processing for generating sound tropism (Manoonpong et al. 2005). Such a reactive controller can even be adapted for manual operation (see extension 2), e.g. by a joystick control, feeding its output signals into the $Input1$ (I_1) and $Input2$ (I_2).

4. Experiments and Results

In the previous section, the artificial perception-action systems have been presented. To test the capability of such systems where they might be affected by unexpected noise and to prove that the systems developed are suitable not only for a simulation but also for a real environment, several experiments were carried out. The first experiment was to measure the limitation of the sensor system in detecting objects with respect to different distances between the sensors and an object as well as different object dimensions. The signal processing network was also tested with the real sensor signals. After this, the physical sensors, neural preprocessing and neural control were all implemented on the physical walking machines to demonstrate the reactive behavior.

4.1. Testing Sensors and Preprocessing

Three different types of IR sensors were chosen to be implemented on the walking machines. They can *physically* detect obstacles at distances between 4 and 30 cm (IR_{type1}), 10 and 80 cm (IR_{type2}) and 20 and 150 cm (IR_{type3})[10] (see also Section 2). IR_{type1} is implemented on the legs of the AMOS-WD06, IR_{type2} is implemented on the front part of the AMOS-WD02 and IR_{type3} is implemented on the front part of the AMOS-WD06. They are used to enable the walking machines to avoid obstacles and to escape from corner and deadlock situations. In order to optimize the performance of the walking machines the valid detection range of each sensor were experimentally tuned. The results are shown in Table 1.

In a further step the minimum surface (width W and height H) of a detectable obstacle was determined for each sensor type. For that, different white square plates having different sizes were placed in front of the sensors at a distance of 6 cm for IR_{type1} and 15 cm for IR_{type2} and IR_{type3}. First, the height of the plate was fixed at 20 cm while the width was varied; then the width was fixed at 20 cm and the height was varied.

10. The information concerning all physical detection ranges is obtained from suppliers' sensor manuals. In fact, the sensors still give usable output signals when the distance between the sensors and an object is closer, i.e. less than 4 cm for IR_{type1}, less than 10 cm for IR_{type2} and less than 20 cm for IR_{type3}.

Table 1. Measured valid detection ranges of the different IR sensors.

Sensor type	Distance
IR_{type1}	2–8 cm
IR_{type2}	8.5–30 cm
IR_{type3}	8.5–30 cm

The experimental set-up is shown in Figure 26 and the results are presented in Tables 2 and 3, where *Yes* indicates that the sensor can detect the obstacle otherwise *No*.

As a result, it turns out that all sensors can detect obstacles having widths $W > 0$ mm and height $H \geq 3$ cm; i.e. good detection is guaranteed at the surface of a detectable obstacle which has to be larger than 30 mm^2. However, because the height of the obstacle in the experiments was measured from the base of the sensor (reference point (see also Figure 26 right)), but the sensors on the machines are at different heights; the AMOS-WD02, for instance, will detect obstacles which are higher than approximately 18 cm above ground. While, the AMOS-WD06 can detect obstacles having height $H \geq 16$ cm (front sensors) and $H \geq 6$ cm (leg sensors).

The last test concerns the neural preprocessing of the sensor signals. Two networks for signal processing were introduced, a standard version using two sensory inputs (compare Figure 12) and a second version using more than two sensory inputs (compare Figure 13). However, only the performance of the standard version is shown here because both networks behave in the same manner. Three tested situations were applied (compare Figure 27). Sensory inputs corresponding to these situations are shown on the left side of Figure 28 and the resulting output signals from the preprocessing network are shown on the right.

The output neurons of the preprocessing network function as on-off switches (compare Figure 28); i.e. an output neuron is switched on ($O \approx +1$) if an obstacle is detected on its side otherwise it switches off ($O \approx -1$). Thus, if both inputs go high as in situation C (see Figure 27C), then both outputs are switched on and the machine walks backwards. If both inputs receive only a medium activation value, only one of the output neurons will be switched on at any one time, as shown in Figure 29. As a result, the network is able to control the behavior of the walking machines in response to the active sensor inputs, i.e. turning away from obstacles and escaping from corner or deadlock situations without getting stuck. This functionality of the network is mainly due to the self-excitatory connections ($W_{self} > 1$) of the output neurons and the strong synapses from the input to the output units (compare Figure 12). An additional property of the resulting hysteresis effect is that sensor signal noise is suppressed. Furthermore, the behavior generated by two simultaneously active medium valued input signals (see Figure 29) is due to the *even loop* of inhibitory connections between the output neurons.

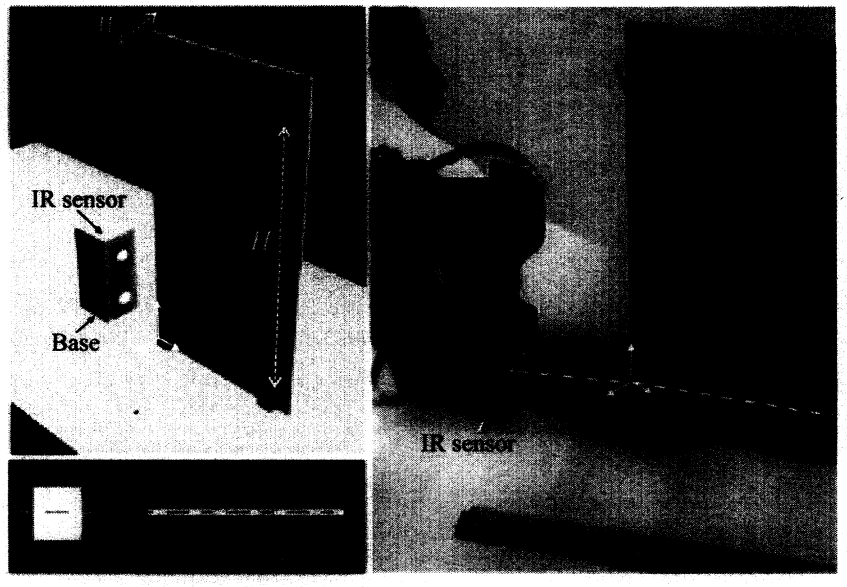

Fig. 26. Left: Drawing of the experimental set-up (upper picture) and its top view (lower picture). Right: Example experimental set-up for testing the sensors installed on the leg of the AMOS-WD06; the same set-up is used for the AMOS-WD02.

Table 2. Ability of sensors to detect obstacles having different widths W and fixed height H = 20 cm.

Sensor type	Distance	< 1 mm	2 mm	3 mm	4 mm	5 mm
IR_{type1}	6 cm	Yes	Yes	Yes	Yes	Yes
IR_{type2}	15 cm	Yes	Yes	Yes	Yes	Yes
IR_{type3}	15 cm	Yes	Yes	Yes	Yes	Yes

Table 3. Ability of sensors to detect obstacles having different heights H with fixed width W = 20 cm.

Sensor type	Distance	1 cm	2 cm	3 cm	4 cm	5 cm
IR_{type1}	6 cm	No	No	Yes	Yes	Yes
IR_{type2}	15 cm	No	No	Yes	Yes	Yes
IR_{type3}	15 cm	No	No	Yes	Yes	Yes

4.2. Obstacle Avoidance Behavior

This section describes experiments carried out to assess the ability of the neurocontroller to generate exploration and obstacle avoidance behaviors. The performance of the obstacle avoidance controller (of the four- and six-legged walking machines) introduced in section 3.4 was first tested in a simulated complex environment (compare Figures 6 and 11 and see also extension 1). It was then loaded into a mobile processor (a PDA) to test the physical walking machines[11]. The simulated walking machines and the physical walking machines apparently behave in a similar way.

11. In the experiment, the AMOS-WD02 performs normal walking (without activating a backbone joint) with a walking cycle at 1.25 s or a walking speed at ≈ 0.45 body length/s (12.7 cm/s) while the AMOS-WD06 has a walking cycle at 1.52 s or a walking speed at ≈ 0.175 body length/s (7 cm/s). With these optimal walking speeds, the walking machines using battery packs can autonomously run for experiments up to 35 minutes.

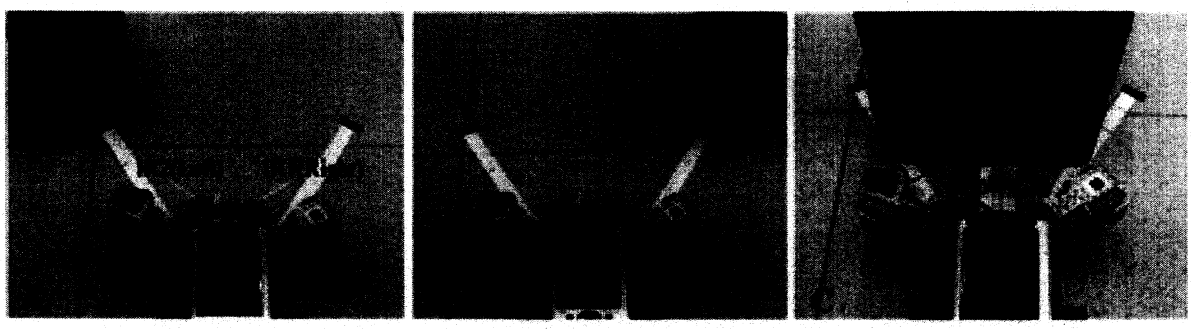

Fig. 27. (A) Situation where objects were presented on the left side in front of the walking machine at a distance of 25 cm. (B) Situation where objects were presented on the right side at the same distance as in (A). (C) Situation where objects were presented on both sides at a closer distance of 10 cm.

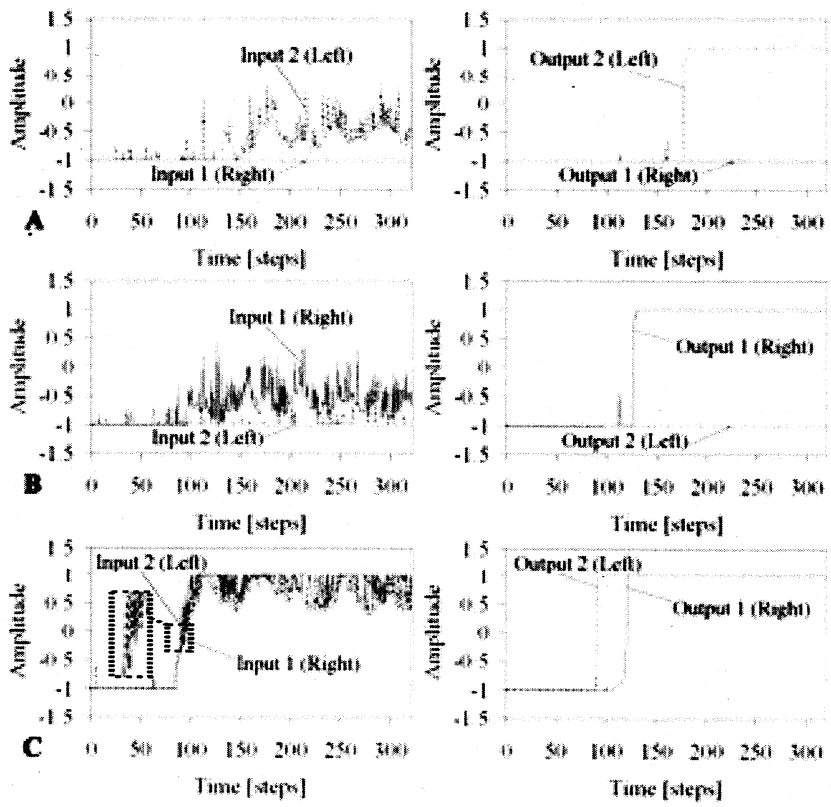

Fig. 28. (A) Situation where objects were fully presented on the left side after around 170 time steps. The left input signal (I_2, dashed line) was active after around that time causing the signal of Output2 (O_2, dashed line) to become active ($\approx +1$) while the signal of Output1 (O_1, solid line) remained inactive (≈ -1). (B) Situation where the objects were fully presented on the right side after around 120 time steps. The right input signal (I_1, solid line) was active after that time, causing O_1 to become active ($\approx +1$) while O_2 remained inactive (≈ -1). (C) Situation where the objects were presented on both sides. Although objects were presented on both sensors at the same time, I_2 was gradually activated to a high level and directly afterwards I_1 was activated to a high level following a similar pattern to I_2. Consequently, O_2 was activated first after around 90 time steps while O_1 became activated after around 120 time steps.

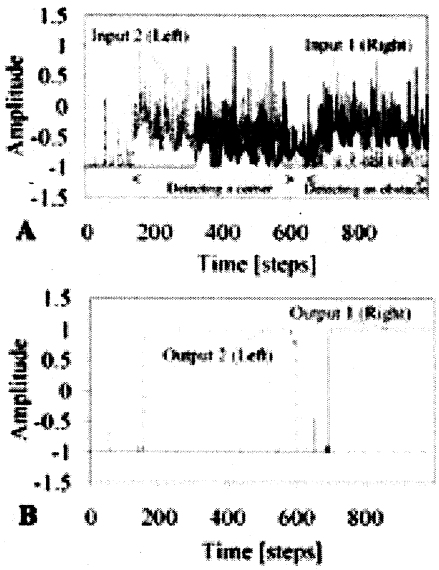

Fig. 29. (A) Input signals of the left (I_2, dashed line) and right (I_1, solid line) sensors. (B) Signals of Output1 (O_1, solid line) and Output2 (O_2, dashed line) correspond to the right and left inputs, respectively. First, the left sensor detected one side of the corner after around 160 time steps, while another side of the corner was also detected by the right sensor after around 300 time steps. Correspondingly, O_2 was excited ($\approx +1$) while O_1 was inhibited (≈ -1). After around 600 time steps, the left sensor did not detect the corner assuming that the machine had already turned right and then walked away from the corner. However, the right sensor was still active assuming that an obstacle was presented on the right side. This caused O_2 to become inactive and O_1 to become active.

The output signals of the neural preprocessing networks were directly connected to the neural control to modify the behavior of the machines. If obstacles are present on either the right side or the left side, the controller will change the rhythmic movement of the legs at the thoracic joints, causing the walking machines to turn away from the obstacles. In some situations, like approaching a corner or a deadlock situation, the preprocessing network determines the turning direction, left or right, with respect to the previously active input signal. For the four-legged walking machine, the obstacle avoidance behavior is illustrated in Figure 30.

It can be seen that Motor0 ($M0$) and Motor1 ($M1$) of the thoracic joints turned in opposite directions if the left sensor ($IR2$) detected an obstacle (compare the left column in Figure 30); correspondingly, Motor2 ($M2$) and Motor3 ($M3$) of the thoracic joints turned in opposite directions when the right sensor ($IR1$) was active (compare the middle column in Figure 30). In special situations, e.g. walking towards a wall or detecting obstacles on both sides, both IR sensors might be simultaneously active. In this case, $M0$, $M1$, $M2$ and $M3$ of the thoracic joints all switched to the opposite directions causing the walking machine to walk backwards (compare the right column in Figure 30). While walking backwards one of the sensors might still be active causing the machine to turn to the corresponding side, eventually leaving the wall. Figure 31 displays a series of photos showing the avoidance of obstacles as well as the machine leaving from a deadlock situation.

However, some difficult situations were experienced in the presents of obstacles like the legs of chairs or desks. To protect the legs of the machine from colliding with these obstacles more sensors should be added on each leg of the machine. Recall that, besides the two sensors in the front, only four sensors were implemented on the four front legs of the AMOS-WD06, one on each leg. The corresponding very effective behavior of AMOS-WD06 under neural control shown in Figure 25 is displayed in Figures 32 and 33. The inversion of the signals at the motor neurons of the thoracic joints ($M3$, $M4$ and $M5$) is shown in Figure 32. There, an obstacle was present for each of the right sensors at different time steps. On the other hand, the signals of the motor neurons ($M0$, $M1$ and $M2$) were inverted when an obstacle was present for each of the left sensors at different time steps (see Figure 33). Figure 34 presents a series of photos of the reactive behavior of the AMOS-WD06.

As demonstrated, the modular reactive neurocontroller (of the four- and six-legged walking machines) successfully accomplishes the obstacle avoidance task. Additionally, the controller can protect the machines from getting stuck in corners or deadlock situations. Thus, due to this functionality, the walking machines can autonomously perform exploration tasks. To see more demonstrations of the behavior of the walking machines, we refer the reader to the video clips (extension 2) at, http://www.chaos.gwdg.de/~poramate/AMOSWD02.html and http://www.chaos.gwdg.de/~poramate/AMOSWD06.html.

5. Discussion

Here, we briefly discuss some remaining issues concerning the walking machines and their neurocontrollers, because most of the relevant discussion points have been treated in the above sections. The proposed walking machines are constructed as mechatronic systems in a straightforward way. Parts of the machines are taken from a construction kit which was developed for the purpose of building different types of walking machines (Breithaupt et al. 2002; Fischer et al. 2004) and for education in the field of robotics.

Concerning the controller, comparable walking machines employ classical control techniques as well as a neural control or a hybrid control (Huber 2000). Classical techniques use, for instance, the subsumption architecture (Brooks 1989) and other AI approaches (Albiez et al. 2003; Ingvast et al. 2003;

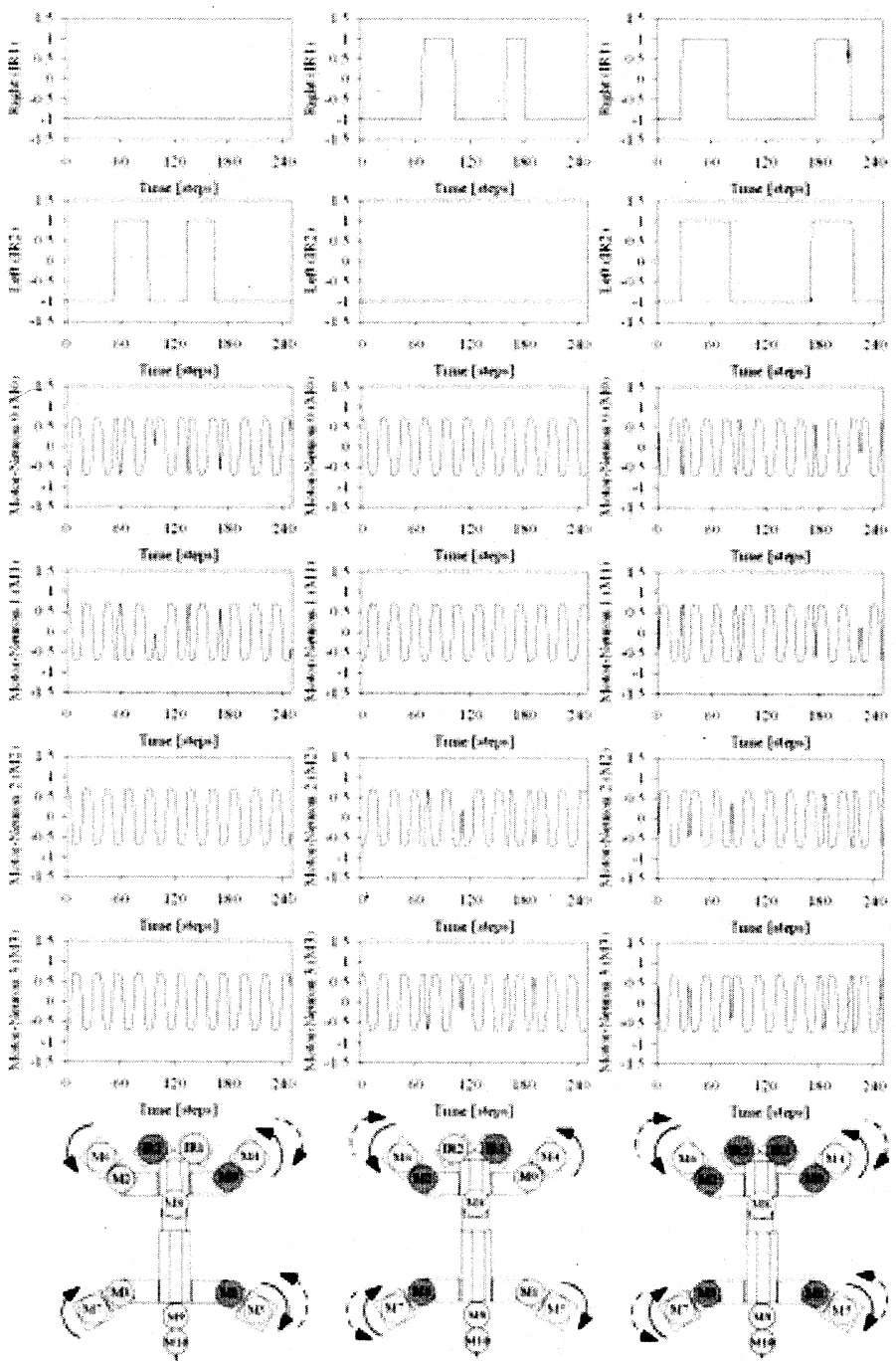

Fig. 30. Left: If obstacles are present on the left side, then the output signals of motor neurons ($M0$, $M1$) on its right change their direction as indicated by the arrow dashed lines in the lower picture. Middle: If obstacles are detected on the right side, then the motors ($M2$, $M3$) on its left run in the reverse direction, indicated again by the arrow dashed lines in the lower picture. Right: In this situation, obstacles are simultaneously detected on both sides resulting in the reversing of all motors ($M0$, $M1$, $M2$ and $M3$). The machine then moves backwards.

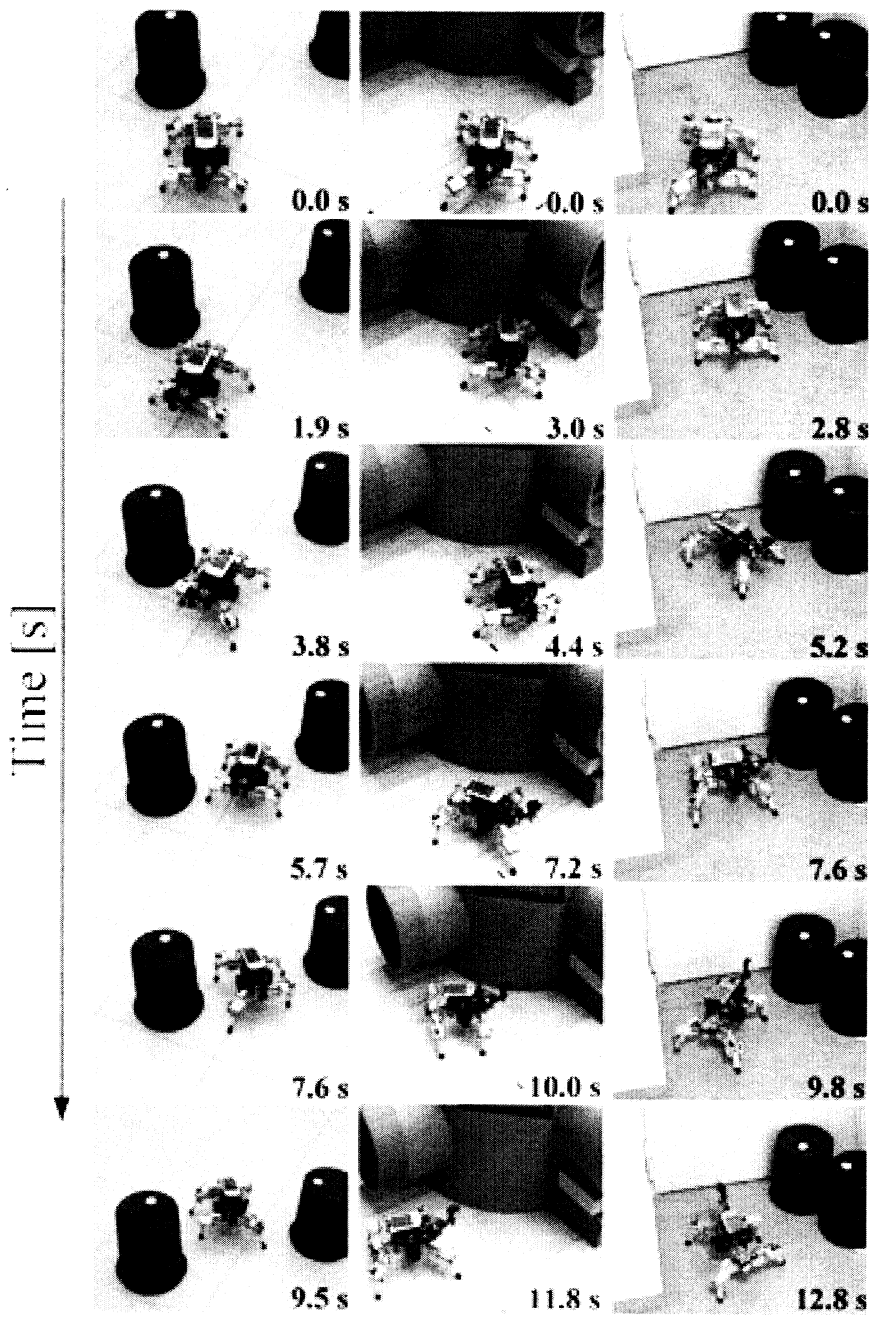

Fig. 31. Examples of the behavior driven by the IR sensors of the four-legged walking machine AMOS-WD02. Left: Typical obstacle avoidance behavior. Middle: Another situation where the walking machine was able to avoid a corner. Comparing the two photos at 3.0 s and 4.4 s, one may observe that the machine is able to slightly step backwards because both sensor signals were active at nearly the same time (at around 3.0 s). While walking backwards (at around 4.4 s), the right sensor was still active while the left sensor was already inactive. Consequently, the walking machine turned left and walked away from the obstacle. Right: The walking machine was also able to escape from a deadlock situation without getting stuck.

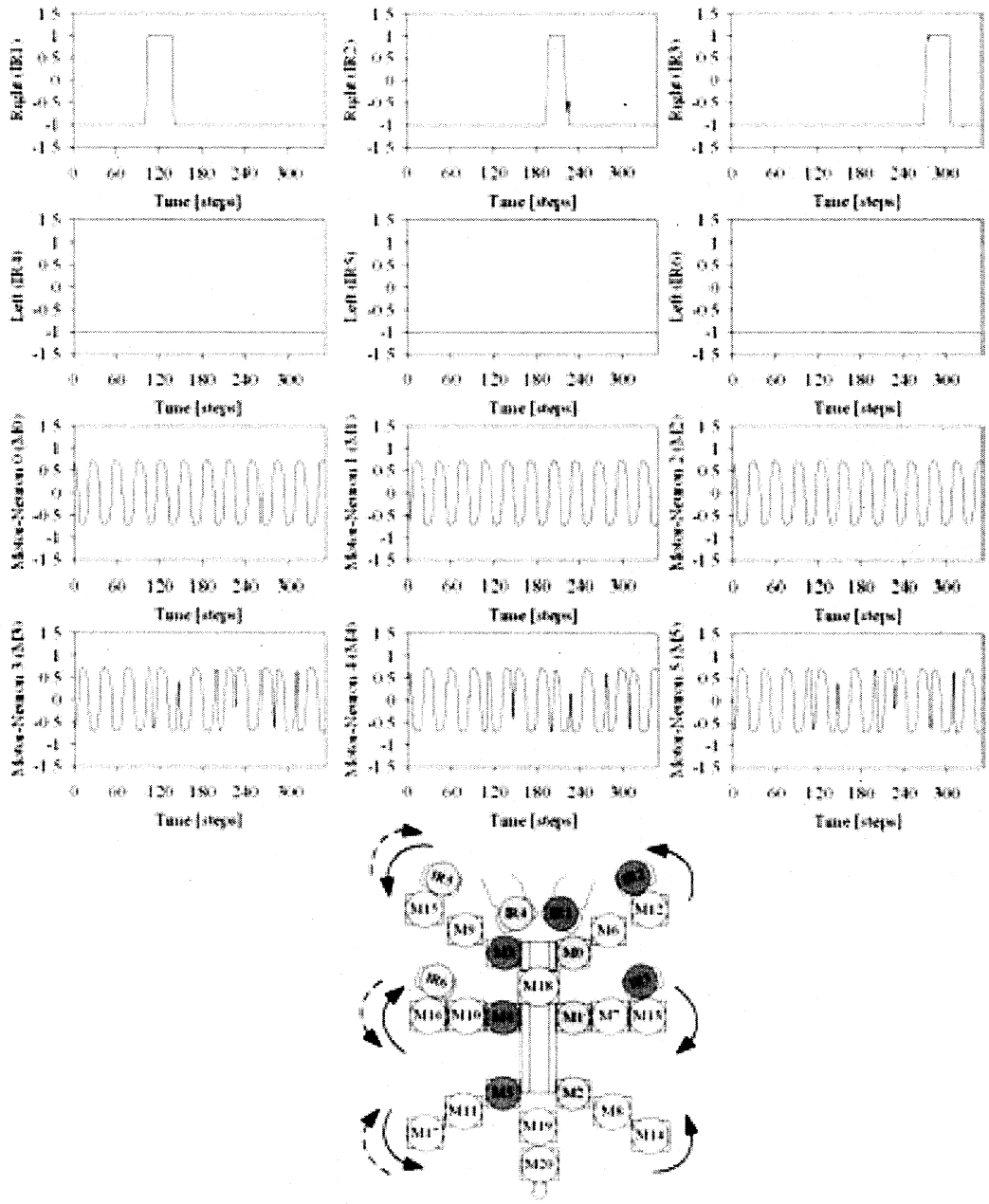

Fig. 32. An obstacle detected by each of the right sensors ($IR1$, $IR2$ and $IR3$) at different time steps; this caused the left motor neurons ($M3$, $M4$ and $M5$) to change to the opposite direction as indicated by the arrow dashed lines in the lower picture. As a result, the walking machine turns left.

Kirchner et al. 2002; Kurazume et al. 2002). Machines like *Tarry I* and *II* use a combination of classical control and neural networks (Cruse et al. 2004). Pure neural network control is applied by Beer et al. (1997), and Parker and Lee (2003). Compared to many of these approaches we emphasize here the embeddedness of neural control; i.e. the controller is imple-

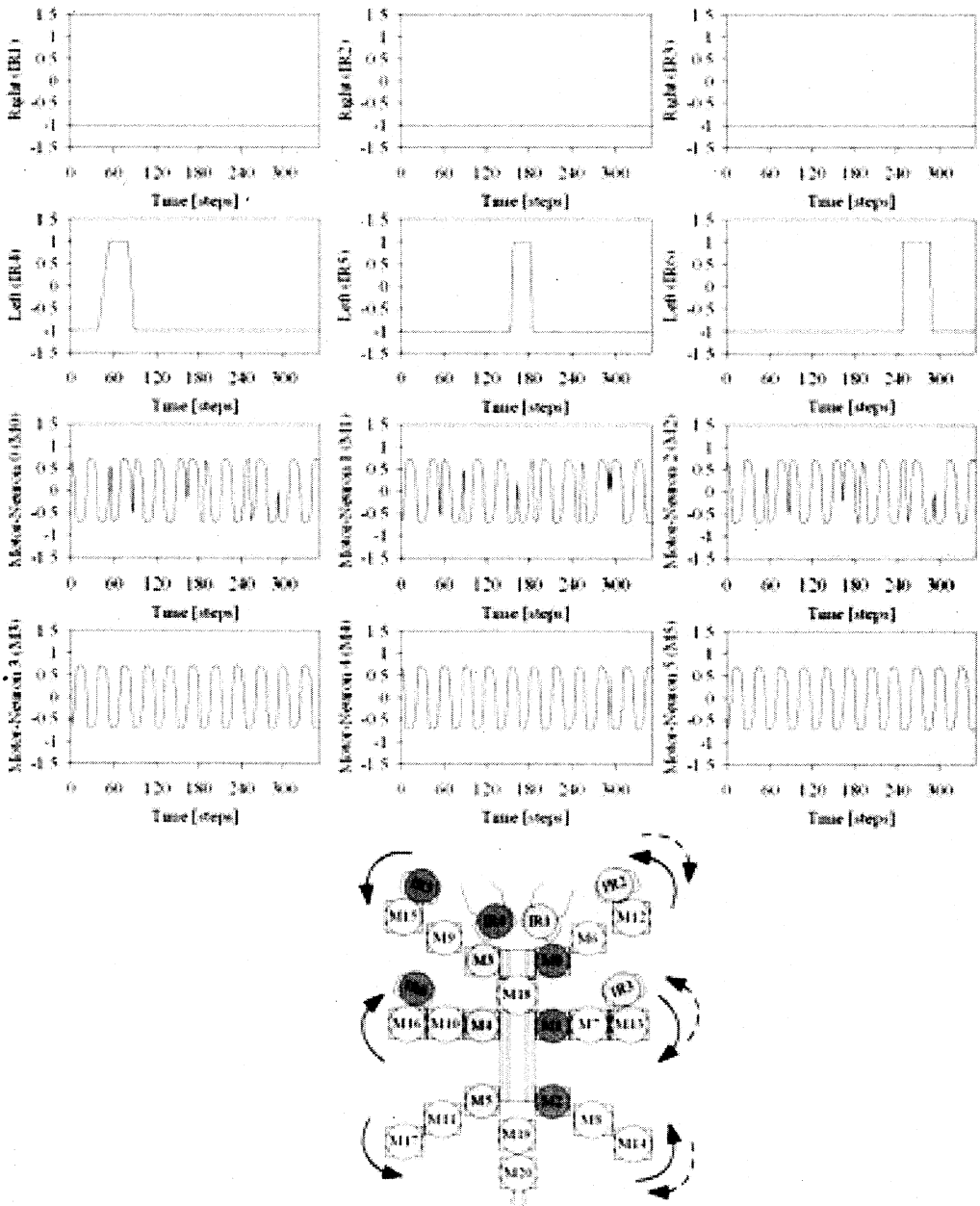

Fig. 33. An obstacle is detected by each of the left sensors ($IR4$, $IR5$ and $IR6$) at different time steps; this causes the right motor neurons ($M0$, $M1$ and $M2$) to change to the opposite direction as indicated by the arrow dashed lines in the lower picture. As a result, the walking machine turns right.

mented on the mobile processor (PDA or microcontroller) of the physical machines.

Most neural control techniques use various types of neural oscillators (Ayers et al. 2000; Matsuoka 1985). For instance, Beer et al. (1997) use a set of six coupled pacemaker (oscillator) neurons where each drives one of the six legs. Others use one oscillator for each degree of freedom (DOF) of the leg joints (Billard and Ijspeert 2000; Tellez et al. 2006). What is

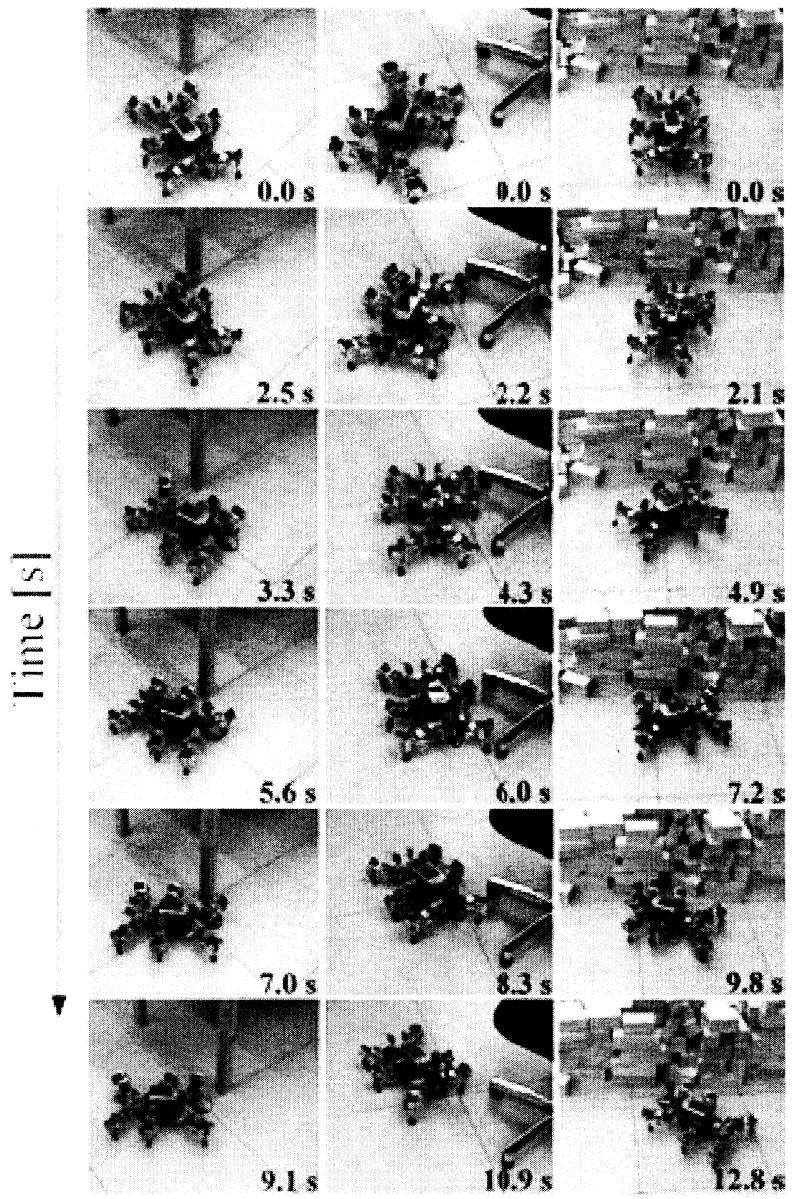

Fig. 34. Examples of the behavior driven by the IR sensors of the six-legged walking machine AMOS-WD06. Left: The walking machine is able to protect its legs from colliding with the leg of the desk, which was detected by the sensors installed on the right legs of the machine. Middle: The machine is also able to avoid the legs of the chair. Right: The walking machine turns away from a large obstacle.

special about the control presented here is that only one simple central pattern generator is used to drive all joints of the walking machines. This central pattern generator uses discrete-time dynamics of a two-neuron network whereas, for instance, Ilg et al. (1999) and Endo et al. (2005) use a continuous-time oscillator, called *Matsuoka Neural Oscillator*, for pattern generation.

In particular, the approach presented here demonstrates that a simple modulation of the central pattern generator signals by appropriately preprocessed sensor signals leads to an effective

reactive behavior of the machines. Although such a simple mechanism will not correspond to biological mechanisms of walking animals, it is shown that it effectively controls the behavior of a machine with many degrees of freedom, e.g. walking machines. It also should be pointed out that all the different walking patterns needed to avoid obstacles, to walk backwards in front of a large object, or even to turn in deadlock situations, are not achieved by changing the control from outside (Kirchner et al. 2002; Cruse et al. 2004). In contrast, they are generated autonomously just by using the corresponding sensory inputs. Of course often proprioceptors (foot contact sensors, joint angle sensors) are used to generate appropriate walking patterns (Albiez et al. 2003; Beer 1990; Cruse et al. 2004; Geng et al. 2006), but here the reactive control is provided by the signals of external sensors (IR sensors).

The functionality of the presented control mechanism is of course not comparable with those found for walking animals, e.g. velocity control is very different. In animals step amplitude is often essentially constant and step frequency is varied (Orlovsky et al. 1999; Ridgel and Ritzmann 2005), while the solution investigated here uses the constant frequency of the central pattern generator and varies the amplitudes. But this can be easily changed, if one wants to be closer to such a biological solution, because the frequency of the SO(2)-network oscillator can be varied by modulating the corresponding parameters (Pasemann et al. 2003) (see Figure 17) in the same way as the amplitudes are varied.

6. Conclusions

This article discusses four- and six-legged walking machines interacting with the physical environment. Their morphologies resemble that of a salamander and a cockroach, respectively. To achieve efficient locomotion, special care has been taken over leg and trunk designs. The machines have been realized as mechatronic systems as well as in physical simulations to test the behavior. The walking patterns, as often found in walking animals (Beer et al. 1993), are generated by a central pattern generator. Here this is realized by using the discrete-time dynamics of a simple two-neuron network.

However, the main interest of this article is not only to demonstrate sensor-driven behavior of the walking machines but also to investigate the analyzable neural mechanisms realizing the desired behavior, e.g. obstacle avoidances. On the basis of a modular neural structure, a controller was built from a combination of neural preprocessing unit and neural control unit. Effective preprocessing of infra-red sensor signals is obtained by a small recurrent neural network, which is also robust against sensor noise. Even more, the recurrent structure is able to generate hysteresis effects which determine turning angles for avoiding obstacles and escaping from deadlock situations. The application of the neural oscillator network together with the velocity regulating network establishes the capability to walk in all directions. The controller was tested and optimized using a physical simulation of the walking machines, and then it was downloaded onto the PDA of the physical walking machines to perform the desired behavior: exploring an unknown environment, avoiding obstacles, and escaping from a deadlock situation.

The proposed modular neurocontroller can easily be adapted to control different kinds of walking machines without changing the internal network structure and its parameters. We want to emphasize that the controller is able not only to control the four- and six-legged walking machines presented here but it can be applied to all even-legged robots, with the restriction that only those gaits can be generated where the diagonal legs are paired and move together. In addition, using different types of sensors the controller can easily be modified to produce, for instance positive tropisms like sound tropism (Manoonpong et al. 2005) or light tropism. Furthermore, the machines can of course be controlled by an operator using joystick signals to mimic the sensor inputs.

Appendix: Index to Multimedia Extensions

The multimedia extension page is found at http://www.ijrr.org.

Table of Multimedia Extensions

Extension	Type	Description
1	Video clip	The reactive behavior of the four and six-legged walking machines (AMOS-WD02 and -WD06) simulated on the physical simulator YARS. The left panel shows the simulated walking machine with its virtual environment. The right panel shows the reactive neurocontroller and the activation of each neuron.
2	Video clip	The physical walking machines (AMOS-WD02 and -WD06) and their reactive behaviors in different environmental situations.

Acknowledgments

The Integrated Structure Evolution Environment (ISEE) software platform for the evolution of recurrent neural networks and Yet Another Robot Simulator (YARS) were kindly provided by Keyan Zahedi, Martin Hülse, and Steffen Wischmann of Fraunhofer AIS.

References

Abushama, F.T. (1964). On the behaviour and sensory physiology of the scorpion Leirus quinquestriatus. *Animal Behaviour*, **12**: 140–153.

Albiez, J.C., Luksch, T., Berns, K., and Dillmann, R. (2003). Reactive reflex based control for a four-legged walking machine. *Robotics and Autonomous Systems*, **443**: 181–189.

Anderson, T.L. and Donath, M. (1988). A computational structure for enforcing reactive behavior in a mobile robot. *Proceedings of the 1988 SPIE Conference on Mobile Robots*, Cambridge, MA, Vol. 1007, pp.198–211.

Arkin, R.C. (1998). *Behavior-based Robotics*, MIT Press, Cambridge, MA.

Ayers, J. (2002). A conservative biomimetic control architecture for autonomous underwater robots. In *Neurotechnology for Biomimetic Robots* (eds J. Ayers, J. Davis and A. Rudolph), pp.241–259, MIT Press, Cambridge, MA.

Ayers, J., Witting, J., McGruer, N., Olcott, C., and Massa, D. (2000). Lobster robots. *Proceedings of the International Symposium on Aqua Biomechanisms*, (eds T. Wu and N. Kato), Tokai University.

Beer, R.D. (1990). *Intelligence as Adaptive Behavior: An Experiment in Computational Neuroethology*, Academic Press, San Diego, CA.

Beer, R.D., Quinn, R.D., Chiel, H.J., and Ritzmann, R.E. (1997). Biologically inspired approaches to robotics: what can we learn from insects? *Communications of the ACM*, **403**: 30–38.

Beer, R.D., Ritzmann, R.E., and McKenna, T. (eds) (1993). *Biological Neural Networks in Invertebrate Neuroethology and Robotics*, Academic Press, Boston, MA.

Berns, K., Cordes, S., and Ilg, W. (1994). Adaptive, neural control architecture for the walking machine LAURON. *Proceedings of the 1994 IEEE/RSJ International Conference on Intelligent Robots and Systems*, Vol. 2, pp.1172–1177.

Berns, K., Ilg, W., Eckert, M., and Dillmann, R. (1998). Mechanical construction and computer architecture of the four-legged walking machine BISAM. *Proceedings of the First International Symposium, CLAWAR' 98*, VRMech 98, Brussels, Belgium, pp.167–72.

Billard, A. and Ijspeert, A.J. (2000). Biologically inspired neural controllers for motor control in a quadruped robot. *Proceedings of the IEEE-INNS-ENNS International Joint Conference on Neural Networks – IJCNN2000*, Vol. 6, pp.637–641.

Breithaupt, R., Dahnke, J., Zahedi, K., Hertzberg, J., and Pasemann, F. (2002). Robo-Salamander: an approach for the benefit of both robotics and biology. *Proceedings of the 5th International Conference on Climbing and Walking Robots, CLAWAR' 02* (ed. P Bedaud), Professional Engineering Publishing, pp.55–62.

Brooks, R.A. (1989). A robot that walks: emergent behaviors from a carefully evolved network. *Neural Computation*, **12**: 253–262.

Brooks, R.A. and Stein, L.A. (1994). Building brains for bodies. *Autonomous Robots*, **11**: 7–25.

Clark, J.E., Cham, J.G., Bailey, S.A., Froehlich, E.M., Nahata, P.K., Full, R.J., and Cutkosky, M.R. (2001). Biomimetic design and fabrication of a hexapedal running robot. *Proceedings of the IEEE International Conference on Robotics and Automation, ICRA*, Vol. 4, pp.3643–3649.

Consi, T.R., Grasso, F., Mountain, D., and Atema, J. (1995). Explorations of turbulent odor plumes with an autonomous underwater robot. *Biological Bulletin*, **189**: 231–232.

Cruse, H. (2002). The functional sense of central oscillations in walking. *Biological Cybernatics*, **864**: 271–280.

Cruse, H., Bläsing, B., Dean, J., Dürr, V., Kindermann, T., Schmitz, J., and Schumm, M. (2004). WalkNet-a decentralized architecture for the control of walking behaviour based on insect studies. In *Walking: Biological and Technological Aspects*, (eds F. Pfeiffer and T. Zielinska), pp. 81–118, CISM Courses and Lectures No. 467. International Centre for Mechanical Sciences, Springer Verlag, Wien, New York.

Dürr, V., Schmitz, J., and Cruse, H. (2004). Behaviour-based modelling of hexapod locomotion: Linking biology and technical application. *Arthropod Structure and Development*, **333**: 237–250.

Endo, G., Nakanishi, J., Morimoto, J., and Cheng, G. (2005). Experimental studies of a neural oscillator for biped locomotion with QRIO. *Proceedings of the IEEE International Conference on Robotics and Automation, ICRA*, Barcelona, Spain, April, pp.596–602.

Fend, M., Yokoi, H., and Pfeifer, R. (2003). Optimal morphology of a biologically-inspired whisker array on an obstacle-avoiding robot. *Proceedings of the 7th European Conference on Artificial Life (ECAL)*, Dortmund, September, pp.771–780.

Filliat, D., Kodjabachian, J., and Meyer, J.A. (1999). Incremental evolution of neural controllers for navigation in a 6-legged robot. *Proceedings of the Fourth International Symposium on Artificial Life and Robotics* (eds Sugisaka and Tanaka), Oita University Press, pp.745–750.

Fischer, J. (2004). A Modulatory Learning Rule for Neural Learning and Metalearning in Real World Robots with Many Degrees of Freedom. PhD thesis, University of Muenster, Shaker Verlag.

Fischer, J., Pasemann, F., and Manoonpong, P. (2004). Neurocontrollers for walking machines – an evolutionary approach to robust behavior. *Proceedings of the 7th International Conference on Climbing and Walking Robots, CLAWAR'04*(eds M. Armada and P. Gonzalez de Santos), pp.97–102.

Floreano, D. and Mondada, F. (1994). Active perception, navigation, homing, and grasping: an autonomous perspective.

From Perception to Action Conference, PERAC'1994 (eds P.H. Gaussier and J.-D. Nicoud), IEEE Computer Society Press, Los Alamitos, CA.

Frik, M., Guddat, M., Karatas, M., and Losch, D.C. (1999). A novel approach to autonomous control of walking machines. *Proceedings of the 2nd International Conference on Climbing and Walking Robots, CLAWAR'99*, Professional Engineering Publishing, Bury St. Edmunds, pp.333–342.

Gaßmann, B., Scholl, K.-U., and Berns, K. (2001). Locomotion of LAURON III in rough terrain. *Proceedings of the IEEE/ASME International Conference on Advanced Intelligent Mechatronics*, Vol. 2, pp.959–964.

Geng, T., Porr, B. and Wörgötter, F. (2006). A reflexive neural network for dynamic biped walking control. *Neural Computation*, **185**: 1156–1196.

Goerke, N., Müller, J., and Brüggemann, B. (2005). SAM: a sensory-actuatory map for mobile robots. *Proceedings of the Third International Symposium on Adaptive Motion in Animals and Machines, AMAM 2005*, ISLE Verlag, Ilmenau.

Hafner, V.V. (2004). Agent-environment interaction in visual homing. *Embodied Artificial Intelligence: International Seminar*, LNCS, Vol. 3139, Springer Verlag, pp.180–185.

Hagras, H., Callaghan, V., and Colley, M.J. (2000). Online learning of fuzzy behaviour co-ordination for autonomous agents using genetic algorithms and real-time interaction with the environment. *Proceedings of The 9th IEEE International Conference on Fuzzy Systems*, Vol. 2, pp.853–858.

Hilljegerdes, J., Spenneberg, D., and Kirchner, F. (2005). The Construction of the Four Legged Prototype Robot ARAMIES. *Proceedings of the 8th International Conference on Climbing and Walking Robots, CLAWAR'05*, London, pp.335–342.

Hooper, S.L. (2000). Central pattern generators. *Current Biology*, **105**: R176–R179.

Huber, M. (2000). A Hybrid Architecture for Adaptive Robot Control. PhD thesis, University of Massachusetts at Amherst.

Hülse, M., and Pasemann, F. (2002). Dynamical neural Schmitt trigger for robot control. *Proceedings of the International Conference on Artificial Neural Networks, ICANN 2002* (ed. J.R. Dorronsoro), LNCS Vol. 2415, Springer Verlag, pp.783–788.

Hülse, M., Wischmann, S., and Pasemann, F. (2004). Structure and function of evolved neuro-controllers for autonomous robots. *Connection Science: Special Issue on Evolutionary Robotics*, **164**: 249–266.

Hülse, M., Zahedi, K., and Pasemann, F. (2003). Representing robot-environment interactions by dynamical features of neuro-controllers. In *Anticipatory Behavior in Adaptive Learning Systems* (eds M. Butz et al.), LNAI Vol. 2684, Springer Verlag, pp.222–242.

Ijspeert, A.J. (2001). A connectionist central pattern generator for the aquatic and terrestrial gaits of a simulated salamander. *Biological Cybernetics*, **845**: 331–348.

Ilg, W., Albiez, J., Jedele, H., Berns, K., and Dillmann, R. (1999). Adaptive periodic movement control for the four-legged walking machine BISAM. *Proceedings of the IEEE International Conference on Robotics and Automation, ICRA*, Vol. 3, pp.2354–2359.

Ingvast, J., Ridderström, C., Hardarson, F. and Wikander, J. (2003). Warp1: Towards walking in rough terrain – control of walking. *Proceedings of the 6th International Conference on Climbing and Walking Robots, CLAWAR'03* (eds G. Muscato and D. Longo), Professional Engineering Publishing.

Jacobi, N. (1998). Running across the reality gap: octopod locomotion evolved in a minimal simulation. *Proceedings of the First European Workshop on Evolutionary Robotics: EvoRobot'98* (eds P. Husbands and J.-A. Meyer), LNCS Vol. 1468, Springer Verlag, pp.39–58.

Kato, K., and Hirose, S. (2001). Development of quadruped walking robot, TITAN-IX -mechanical design concept and application for the humanitarian de-mining robot. *Advanced Robotics*, **152**: 191–204.

Kerscher, T., Albiez, J., and Berns, K. (2002). Joint control of the six-legged robot AirBug driven by fluidic muscles. *Proceedings of the Third International Workshop on Robot Motion and Control, RoMoCo'02*, Bukowy Dorek, Poland, November, pp. 27–32.

Kimura, H., and Fukuoka, Y. (2004). Adaptive walking of a quadruped robot in outdoor environment based on biological concepts. *Proceedings of the 9th International Symposium on Experimental Robotics, ISER2004*, Singapore, ID-132.

Kirchner, F., Spenneberg, D., and Linnemann, R. (2002). A biologically inspired approach toward robust real-world locomotion in legged robots. In *Neurotechnology for Biomimetic Robots* (eds J. Ayers, J. Davis and A. Rudolph), pp. 419–447, MIT Press, MA.

Kurazume, R., Yoneda, K., and Hirose, S. (2002). Feedforward and feedback dynamic trot gait control for quadruped walking vehicle. *Autonomous Robots*, **122**: 157–172.

Lewis, M.A., Tenore, F., and Etienne-Cummings, R. (2005). CPG design using inhibitory networks. *Proceedings of the IEEE International Conference on Robotics and Automation, ICRA*, Barcelona, Spain.

Manoonpong, P., Pasemann, F., and Fischer, J. (2004). Neural processing of auditory-tactile sensor data to perform reactive behavior of walking machines. *Proceedings of the IEEE International Conference on Mechatronics and Robotics*, Vol. 1, pp. 189–194.

Manoonpong, P., Pasemann, F., Fischer, J., and Roth, H. (2005). Neural processing of auditory signals and modular neural control for sound tropism of walking machines. *In-*

ternational Journal of Advanced Robotic Systems, **23**: 223–234.

Marder, E., and Calabrese, R.L. (1996). Principles of rhythmic motor pattern production. *Physiological Reviews*, **76**: 687–717.

Markelic, I. (2005). Evolving a neurocontroller for a fast quadrupedal walking behavior. Master thesis, Institut für Computervisualistik Arbeitsgruppe Aktives Sehen, Universität Koblenz-Landau.

Matsuoka, K. (1985). Sustained oscillations generated by mutually inhibiting neurons with adaptation. *Biological Cybernetics*, **526**: 367–376.

Mondada, F., Franzi, E., and Ienne, P. (1993). Mobile robot miniaturisation: A tool for investigation in control algorithms. *Proceedings of the Third International Symposium on Experimental Robotics*, Kyoto, Japan, October, pp.501–513.

Moravec, H.P. (1977). Towards automatic visual obstacle avoidance. *Proceedings of the 5th International Joint Conference on Artificial Intelligence*, Cambridge, MA, pp.584–590.

Nakada, K., Asai, T., and Amemiya, Y. (2003). An analog neural oscillator circuit for locomotion control in quadruped walking robot. *Proceedings of the International Joint Conference on Neural Networks*, Vol. 2, pp.983–988.

Nehmzow, U., and Walker, K. (2003). Quantitative description of robot-environment interaction using chaos theory. *Proceedings of European Conference on Mobile Robotics, ECMR*, Warsaw.

Nilsson, N.J. (1969). A mobile automaton: An application of artificial intelligence techniques. *Proceedings of the 1st International Joint Conference on Artificial Intelligence*, Washington DC, pp. 509–520.

Nolfi, S. and Floreano, D. (1998). Coevolving predator and prey robots: do 'Arms Races' arise in artificial evolution? *Artificial Life*, **44**: 311–335.

Okada, M., Nakamura, D., and Nakamura, Y. (2003). Hierarchical design of dynamics based information processing system for humanoid motion generation. *Proceedings of the 2nd International Symposium on Adaptive Motion of Animals and Machines, AMAM2003*, Kyoto, SaP-III-1.

Orlovsky, G.N., Deliagina, T.G., and Grillner, S. (1999). *Neural Control of Locomotion. From Mollusk to Man*, Oxford University Press.

Parker, G.B., and Lee, Z. (2003). Evolving neural networks for hexapod leg controllers. *Proceedings of the 2003 IEEE/RSJ International Conference on Intelligent Robots and Systems*, Vol. 2, pp.1376–1381.

Pasemann, F. (2002). Complex dynamics and the structure of small neural networks. *Network: Computation in Neural Systems*, **132**: 195–216.

Pasemann, F. (1993). Discrete dynamics of two neuron networks. *Open Systems and Information Dynamics*, **2**: 49–66.

Pasemann, F., Hild, M., and Zahedi, K. (2003). SO(2)-networks as neural oscillators. *Computational Methods in Neural Modeling: Proceedings of the 7th International Work-Conference on Artificial and Natural Networks, IWANN 2003* (eds J. Mira J.R. and Alvarez), LNCS Vol. 2686, Springer, Berlin, pp. 144–151.

Payton, D.W. (1986). An architecture for reflexive autonomous vehicle control. *Proceedings of the IEEE International Conference on Robotics and Automation, ICRA*, San Francisco, CA, pp.1838–1845.

Pfeifer, R. and Scheier, C. (1999). *Understanding Intelligence*, MIT Press, Cambridge, MA.

Quinn, R.D., Nelson, G.M., Bachmann, R.J., Kingsley, D.A., Offi, J., and Ritzmann, R.E. (2001). Insect designs for improved robot mobility. *Proceedings of the 4th International Conference on Climbing and Walking Robots, CLAWAR'01* (eds K. Berns and R. Dillmann), Professional Engineering Publishing, pp.69–76.

Reeve, R. (1999). Generating walking behaviours in legged robots. PhD thesis, University of Edinburgh, Scotland, UK.

Ridgel, A.L. and Ritzmann, R.E. (2005). Effects of neck and circumoesophaegeal connective lesions on posture and locomotion in the cockroach. *Journal of Comparative Physiology. A: Neuroethology, Sensory, Neural, and Behavioral Physiology*, **1916**: 559–573.

Righetti, L., and Ijspeert, A.J. (2006). Programmable central pattern generators: an application to biped locomotion control. *Proceedings of the IEEE International Conference on Robotics and Automation, ICRA*, Orlando, FL, pp.1585–1590.

Ritzmann, R.E., Quinn, R.D., and Fischer, M.S. (2004). Convergent evolution and locomotion through complex terrain by insects, vertebrates and robots. *Arthropod Structure and Development*, **333**: 361–379.

Schmucker, U., Schneider, A., Rusin, V., and Zavgorodniy, Y. (2005). Force sensing for walking robots. *Proceedings of the Third International Symposium on Adaptive Motion in Animals and Machines, AMAM 2005*, ISLE Verlag, Ilmenau.

Smith, R. (2004). Open Dynamics Engine v0.5 User Guide, http://ode.org/ode-0.5-userguide.html.

Spenneberg, D. and Kirchner, F. (2002). SCORPION: a biomimetic walking robot. *Robotik 2002*, VDI-Bericht, Vol. 1679, pp. 677–682.

Stein, P.S.G, Grillner, S., Selverston, A.I., and Stuart, D.G. (1997). *Neurons, Networks, and Behavior*, MIT Pres, Cambridge, MA.

Taga, G., Yamaguchi, Y., and Shimizu, H. (1991). Self-organized control of bipedal locomotion by neural oscillators in unpredictable environment. *Biological Cybernetics*, **653**: 147–159.

Téllez, R., Angulo, C., and Pardo, D. (2006). Evolving the walking behaviour of a 12 DOF quadruped using a distributed neural architecture. *Proceedings of the 2nd Inter-*

national Workshop on Biologically Inspired Approaches to Advanced Information Technology, Bio-ADIT'2006, LNCS Vol. 3853, Springer, pp.5–19.

Webb, B. (2000). What does robotics offer animal behaviour? *Animal Behaviour*, **605**: 545–558.

Wei, T.E., Quinn, R.D., and Ritzmann, R.E. (2004). CLAWAR that benefits from abstracted cockroach locomotion principles. *Proceedings of the 7th International Conference on Climbing and Walking Robots, CLAWAR'04)* (eds M. Armada and P. Gonzalez de Santos), Madrid, Spain.

Wischmann, S., Hülse, M., Knabe, J., and Pasemann, F. (2006). Synchronization of internal neural rhythms in multi-robotic systems. *Adaptive Behavior*, **142**: 117–127.

Yamaguchi, T., Watanabe, K., and Izumi, K. (2005). Neural network approach to acquiring free-gait motion of quadruped robots in obstacle avoidance. *Artificial Life and Robotics*, **94**: 188–193.

Yoneda, K., Ota, Y., Ito, F., and Hirose, S. (2001). Quadruped walking robot with reduced degrees of freedom. *Journal of Robotics and Mechatoronics*, **132**: 190–197.